Virology 572 (2022) 1–16

Contents lists available at ScienceDirect

Virology

journal homepage: www.elsevier.com/locate/virology

Key tethering function of Atg11 autophagy scaffold protein in formation of virus-induced membrane contact sites during tombusvirus replication

Yuanrong Kang [1], Wenwu Lin [1], Yuyan Liu, Peter D. Nagy [*]

Department of Plant Pathology, University of Kentucky, Lexington, KY, 40546, USA

A B S T R A C T

Positive-strand RNA viruses induce the biogenesis of viral replication organelles (VROs), which support viral replication in infected cells. VRO formation requires viral replication proteins, co-opted host factors and intracellular membranes. Here, we show that the conserved Atg11 autophagy scaffold protein is co-opted by Tomato bushy stunt virus (TBSV) via direct interactions with the viral replication proteins. Deletion of *ATG11* in yeast or knockdown of the homologous Atg11 in plants led to reduced tombusvirus replication, thus indicating pro-viral function for Atg11. Based on co-purification, BiFC and proximity-labeling experiments, we find that Atg11 is co-opted to stabilize virus-induced membrane contact sites (vMCS) within VROs. We propose that the tethering and scaffold function of Atg11 is critical in vMCSs for lipid enrichment. Absence of Atg11 interferes with sterols enrichment in VROs, rendering VROs RNAi-sensitive. Altogether, the expanding roles of co-opted host proteins with tethering functions suggest that the tombusvirus VROs are elaborate structures.

1. Introduction

Positive-strand (+)RNA viruses of eukaryotic organisms have small genomes and they have to co-opt numerous host factors to support their replication inside the infected cells. Virus replication depends on the biogenesis of viral replication organelles (VROs), which cluster many membrane-bound viral replicase complexes (VRCs) (Altan-Bonnet, 2017; Belov and van Kuppeveld, 2012; Fernandez de Castro et al., 2016; Garcia-Ruiz, 2018; Hyodo and Okuno, 2020; Mäkinen et al., 2017; Nagy and Pogany, 2012; Wang, 2015). VRO biogenesis requires membrane deformation, new lipid biosynthesis, phospholipid and sterol transfer and co-opting vesicular trafficking (Altan-Bonnet, 2017; Nagy and Feng, 2021; Paul and Bartenschlager, 2015; Schoggins and Randall, 2013; Zhang et al., 2019). The membranous VROs sequester the viral (+)RNA and viral and co-opted host proteins for efficient replication. In addition, VROs also protect the viral (+)RNA and the dsRNA replication intermediate from recognition and elimination by the host innate immune system (Jin et al., 2018; Kovalev et al., 2017; Shulla and Randall, 2016). The VROs coordinate the viral replication process spatiotemporally (Altan-Bonnet, 2017; Hsu et al., 2010; Schoggins and Randall, 2013; Wang et al., 2011).

Tomato bushy stunt virus (TBSV), which is a small (+)RNA virus of plants, is studied intensively to unravel the basic mechanism of viral RNA replication (Gunawardene et al., 2017; Nagy, 2016, 2020; Nicholson and White, 2014). TBSV codes for two essential replication proteins, the p92 RdRp and the p33 replication protein, which is the master regulator of VRO assembly and viral (+)RNA recruitment into VRCs (Pogany et al., 2005; Xu and Nagy, 2017). TBSV replicon (rep)RNA replicates in the surrogate host yeast (*Saccharomyces cerevisiae*) to a high level (Nagy, 2016, 2017; Nagy et al., 2014). Yeast-based genome-wide and proteome-wide studies with TBSV led to the identification of numerous host factors co-opted for viral RNA replication and recombination (Kovalev et al., 2019; Nagy, 2016; Nagy and Pogany, 2012; Prasanth et al., 2016; Xu and Nagy, 2014). Overall, TBSV depends on global phospholipid and sterol biosynthesis (Chuang et al., 2014; Sharma et al., 2010, 2011). Formation of VRCs and activation of the viral-coded p92 RdRp requires phosphatidylethanolamine (PE), phosphoinositides and sterols (Feng et al., 2019; Kovalev et al., 2020; Pogany and Nagy, 2012, 2015; Sasvari et al., 2020; Xu and Nagy, 2015, 2016, 2017).

TBSV induces subcellular membrane proliferation and peroxisome aggregation in both yeast and plant cells. One of the characteristic features of TBSV infection is the formation of virus-induced membrane contact sites (vMCSs) (Barajas et al., 2014b; Fernandez de Castro et al., 2017; Nagy, 2016; Nagy et al., 2016). vMCS forms between the hijacked subdomain in the ER and the peroxisome with the help of p33 replication protein and co-opted host proteins. For example, a group of oxystrerol-binding proteins (OSBP in mammals, Osh proteins in yeast, and ORP proteins in plants) and ER-resident VAP (VAMP-associated protein, Scs2 in yeast, VAP27-1, VAP27-2 and PVA12 proteins in plants)

* Corresponding author.
E-mail address: pdnagy2@uky.edu (P.D. Nagy).
[1] These authors contributed equally.

https://doi.org/10.1016/j.virol.2022.04.007
Received 15 February 2022; Received in revised form 15 April 2022; Accepted 25 April 2022
Available online 29 April 2022
0042-6822/

are critical for vMCS formation/function, which are essential for the enrichment of sterols and phosphoinositides within VROs (Barajas et al., 2014b). In the absence of sterol or phosphoinositide enrichment within VROs, tombusvirus p33 replication protein becomes sensitive to proteasomal degradation (Feng et al., 2019; Xu and Nagy, 2017). The cytosolic Osh/ORP proteins and the ER-resident VAP proteins must be recruited to vMCSs via protein-protein interactions with p33 replication protein (Barajas et al., 2014b). A subdomain of ER, called ERAS (ER arrival site for COPI vesicles), is important for vMCS formation. The main co-opted component of ERAS is the SNARE complex, including the syntaxin18-like Ufe1 and Use1 proteins (Sasvari et al., 2013, 2018). Another critical host protein in vMCS formation/function is the ER-resident Sac1 PI4P phosphatase, which is needed for the directional transfer of sterols from the ER to the acceptor membranes through converting PI(4)P phosphoinositide to PI phosphatidylinositol (Sasvari et al., 2020). PI(4)P is used by oxysterol binding proteins to exchange for sterol/oxysterols/ergosterols to allow transfer of these lipids at the MCS (Henne, 2016; Jackson et al., 2016; Mesmin and Antonny, 2016; Olkkonen and Li, 2013; Raiborg et al., 2016). The acceptor membranes (i.e., peroxisomal membrane for TBSV and mitochondrial membrane for CIRV) are recruited into vMCS by TBSV p33/CIRV p36 replication proteins and co-opted Fis1 mitochondrial fission protein (Lin et al., 2021). In spite of its significance in VRO biogenesis, the complete protein composition of vMCS is not yet known.

Role of the Atg11 adapter and scaffolding protein in selective autophagy, such as pexophagy and mitophagy, is to direct the cargo proteins and autophagy receptors to the phagophore assembly site (PAS), recruit selected group of proteins to PAS in yeast and to tether Atg9 vesicles (Delorme-Axford and Klionsky, 2015; Fukuda and Kanki, 2018; Matscheko et al., 2019; Oku and Sakai, 2016; Yokota et al., 2017). Atg11 is an important hub that coordinates cargo selection, membrane trafficking, membrane tethering, stabilize membrane curvature, and required for membrane expansion of the autophagosome (Eickhorst et al., 2020; Zientara-Rytter and Subramani, 2020). Moreover, Atg11 is a large conserved protein (protein with comparable functions is called FIP200, also called RBCC1 in mammals) with an ortholog in *Arabidopsis thaliana* and other plants, and it is expressed during normal (stationary) conditions (Backues and Klionsky, 2012; Delorme-Axford and Klionsky, 2015; Kang et al., 2018; Li and Vierstra, 2014).

We decided to characterize the molecular function of Atg11 during TBSV replication. We based our initial model on Atg11 putative function in TBSV replication on the known features of Atg11, including interaction with Fis1 mitochondrial fission protein, which has been shown as a co-opted tethering protein during vMCS formation (Lin et al., 2021; Mao et al., 2013). Atg11 also interacts with other characterized pro-viral host proteins, such as Vps34 PI3P kinase, and Ypt1 (Rab1), Vps21 (Rab5) and Ypt7 (Rab7) small GTPases, all of which are recruited by TBSV for functions within the VROs (Feng et al., 2019, 2021; Inaba and Nagy, 2018; Nagy, 2016; Xu and Nagy, 2016). These features place Atg11 as a likely candidate to tether these host factors and membranes and act as an assembly platform in VROs. Indeed, we find that Atg11 is co-opted by the TBSV p33 replication protein into VROs formed from clustered peroxisomes. Atg11 also binds to the p36 replication protein of the closely-related carnation Italian ringspot virus (CIRV) in VROs formed from clustered mitochondria. Instead of the canonical function as a selective autophagy scaffold protein, Atg11 is found to play a pro-viral role in facilitating the formation of vMCS. This function of Atg11 is likely performed in collaboration with the p33/p36 replication protein and co-opted cellular vMCS proteins, such as the ER-resident Scs2/VAP27 VAP tethering proteins, the oxysterol-binding proteins (Osh6 and ORP3), Sac1 PI4P phosphatase and Fis1 mitochondrial fission protein within VROs. We propose that Atg11 serves as a co-opted tethering protein to facilitate the stable formation of vMCSs involving peroxisomes and the ER membrane for TBSV and mitochondria and the ER membrane in case of CIRV. Thus, tombusviruses usurp a key selective autophagy protein for pro-viral functions. Altogether, co-opting Atg11 is critical for tombusvirus VRO biogenesis in yeast and plant cells.

2. Results

Atg11 autophagy scaffold protein is required for tombusvirus replication. Based on known interaction of Atg11 with Fis1 mitochondrial fission protein and Vps34 PI3K, which are key co-opted pro-TBSV host factors (Feng et al., 2019; Lin et al., 2021), and other co-opted host proteins (Nagy, 2017, 2020), Atg11 has emerged as a highly connected putative candidate for TBSV replication. To test the effect of Atg11 on TBSV replication, we expressed tombusvirus p33 and $p92^{pol}$ replication proteins and the replicon (rep)RNA in haploid yeast with *ATG11* deletion. Northern blot analysis of repRNA level revealed ~4-fold reduced accumulation of TBSV and the closely-related cucumber necrosis virus (CNV) in atg11Δ yeast in comparison with the WT yeast (Fig. 1A–B). Similar to TBSV and CNV, both of which replicate using the peroxisomal membrane surfaces, the mitochondria-associated CIRV, a closely-related tombusvirus, replication was also greatly reduced in atg11Δ yeast (Fig. 1C). Plasmid-based expression of WT Atg11 partially complemented CNV and CIRV replication in yeast (Fig. 1C–D). Remarkably, the expression level of TBSV and CNV p33 and the CIRV p36 replication proteins was also reduced in atg11Δ yeast (Fig. 1). In addition, over-expression of Atg11 enhanced CIRV replication and the accumulation of p36 replication protein in WT yeast (Fig. 1C, lanes 4–6 versus 1–3). These data suggest that Atg11 is critical for tombusvirus replication in different subcellular niches. Because of the observed major effect of Atg11 on the replication of tombusviruses in yeast, Atg11 emerges as a new pro-viral host factor whose function is characterized in more details below.

Atg11 autophagy-related protein has pro-viral functions in plants. Atg11 is a large protein in *Arabidopsis* with two predicted domains (Supplementary Fig. S1), whose function is not yet characterized in detail in plants (Kang et al., 2018; Li and Vierstra, 2014). The two Atg11 proteins are highly similar in *Nicotiana benthamiana* plants (Supplementary Fig. S1). To study if tombusviruses depend on Atg11 functions in plants, first we tested if Atg11 expression is affected during TBSV infection in *Nicotiana benthamiana* plants. Semi-quantitative RT-PCR and RT-qPCR analyses of Atg11 mRNA levels in TBSV-infected versus mock-treated *N. benthamiana* leaves revealed up-regulation of Atg11 mRNA level in the TBSV inoculated leaves 2 days after inoculation (dpi), whereas no differences were seen after 1 dpi (Fig. 2A, lanes 7–9 versus 10–12 and the RT-qPCR graph, bottom panel). Interestingly, Atg11 mRNA level also increased in the systemically-infected leaves at 4 and 5 dpi (Fig. 2A, lanes 13–15 versus 16–18 and the RT-qPCR graph, bottom panel), suggesting that TBSV replication induces high level of Atg11 expression in *N. benthamiana* plants.

Second, we silenced Atg11 expression based on virus-induced gene-silencing (VIGS) in *N. benthamiana* plants. We selected two regions in *NbATG11*, which are almost identical in both *NbATG11* genes (Supplementary Fig. S2). VIGS-based knockdown of Atg11 in *N. benthamiana* led to ~2-to-3-fold reduction of $CNV^{20KStop}$ (not expressing the gene silencing suppressor protein), TBSV and CIRV RNAs, respectively, in the inoculated leaves (Fig. 2B–D). Knockdown of Atg11 level did not cause obvious phenotype in *N. benthamiana*. Third, expression of the NbAtg11 in *N. benthamiana* plants increased $CNV^{20KStop}$ and CIRV RNA accumulation (Fig. 2E–F). Altogether, these data confirmed the pro-viral role of Atg11 in supporting tombusvirus replication in yeast and plants.

Recruitment of Atg11 into VROs in plants. To analyze if Atg11 is co-opted by TBSV into large VROs, we co-expressed RFP-tagged Atg11 with BFP-tagged TBSV p33 replication protein and GFP-SKL peroxisomal marker protein in *N. benthamiana* cells infected with TBSV, followed by confocal imaging. We found a high level of co-localization of TBSV p33 replication protein and Atg11 within VROs consisting of aggregated peroxisomes (Fig. 3A, top two panels). We noted that Atg11 was present in a portion of the VROs based on comparison of distribution of p33 and Atg11 punctate structures (Fig. 3A). Interestingly, the expression of p33

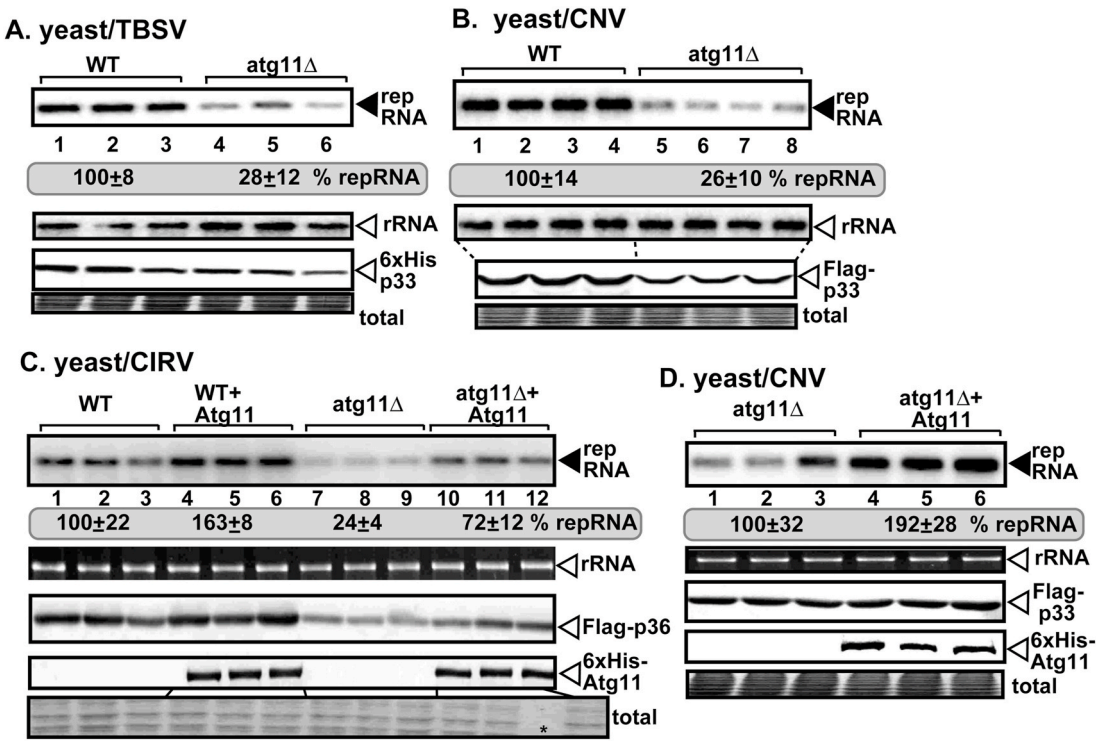

Fig. 1. Atg11 autophagy scaffold protein is an essential host factor for tombusvirus replication in yeast. (A–B) Deletion of *ATG11* inhibits TBSV, and CNV RNA replication in yeast. Top panels: northern blot analyses of repRNA using a 3′ end specific probe demonstrate reduced accumulation of repRNA in atg11Δ yeast strain in comparison with the WT (BY4741) yeast strain. The replication proteins His_6-p33 and His_6-$p92^{pol}$ of TBSV were expressed from plasmids from the galactose-inducible *GAL1* promoter, whereas the Flag-p33 and Flag-p92 of CNV were expressed from plasmids from the copper-inducible *CUP1* promoter. The DI-72 (+) replicon (rep)RNA was expressed from the *GAL10* promoter. Second panel: northern blot with 18S ribosomal RNA specific probe was used as a loading control. Bottom images: western blot analysis of the level of His_6-tagged proteins and Flag-tagged proteins with anti-His or anti-Flag-antibodies, respectively. Coomassie blue-stained SDS-PAGE was used as protein loading control. (C) Deletion of *ATG11* inhibits CIRV replication in yeast. Top panel: northern blot analyses of repRNA The CIRV Flag-p36 and Flag-$p95^{pol}$ were expressed from plasmids from the *CUP1* promoter. His_6-Atg11 was expressed from the *GAL1* promoter from a plasmid. See further details in panel A–B. (D) Complementation of atg11Δ yeast strain with plasmid-borne Atg11 enhances CNV replication. His_6-Atg11 was expressed from the *GAL1* promoter from a plasmid. See further details in panel A–B. Each experiment was repeated three times.

replication protein without TBSV infection led to the recruitment of Atg11 into VRO-like structures to comparable extent as the actively replicating TBSV did (Fig. 3A). Note that the expression of TBSV p33 alone results in VRO-like structures with numerous aggregated peroxisomes, similar to VROs during TBSV infection (Barajas et al., 2014a). In the absence of viral components, Atg11 did not localize to peroxisomes in plants (Fig. 3A, bottom panel). Expression of only the yeast Atg11-like domain of the NbAtg11 (termed R2) also resulted in co-localization with p33-BFP within VROs in *N. benthamiana* (Fig. 3B).

Similar confocal microscopy-based experiments with the closely-related CIRV, which builds VROs using clustered mitochondria, revealed the high extent of co-localization of RFP-Atg11 with the CIRV p36-BFP replication protein and GFP-Tim21 mitochondrial membrane protein (Fig. 3C, top panel). The localization pattern of Atg11 within the VROs during CIRV infection was similar to the pattern observed with TBSV infection (compare Fig. 3A and C). In the absence of CIRV replication, Atg11 did not colocalize with mitochondrial marker in *N. benthamiana* (Fig. 3C). These data suggest that Atg11 is recruited into the large CIRV VROs with the help of the viral p36 replication protein in plant cells. Based on these experiments, we conclude that Atg11 autophagy-related protein is efficiently recruited by the TBSV p33 and the CIRV p36 replication proteins to VROs in *N. benthamiana*.

Tombusvirus replication proteins interact with Atg11 *in vitro* and in yeast and plants. To test if Atg11 interacts with the tombusvirus replication proteins, we Flag-affinity purified the TBSV replication proteins from yeast expressing His_6-tagged Atg11. The yeast membranous fraction containing the TBSV replicase was detergent-solubilized, followed by Flag-purification of the tombusvirus replicase. These experiments confirmed the presence of Atg11 in the purified replicase preparations, which are active *in vitro* (Fig. 4A see also Fig. S3A).

To confirm direct interactions between TBSV p33 and Atg11 protein, we used a pull-down assay with MBP-tagged p33 and GST-His_6-tagged Atg11 proteins affinity-purified from *E. coli* (Fig. 4B). Similar interaction studies were performed with the CIRV p36 replication protein using the pull-down assay (Fig. 4B). For the pull-down assay, we used truncated TBSV p33 and CIRV p36 replication proteins missing the N-terminal and the membrane-binding regions to aid their solubility in *E. coli* (Fig. 4B). Altogether, the pull-down data show that the TBSV and CIRV replication proteins bind to Atg11 host protein *in vitro*, and the C-terminal domains of the replication proteins facing the cytosolic compartment is involved in binding to Atg11 (Fig. 4B).

To provide additional evidence for the interaction between the TBSV p33 replication protein and Atg11 *in vivo*, we used protein proximity-labeling approach based on *E. coli*-derived BirA biotin-ligase and Avi-Tag, which serves as a biotin acceptor peptide (Fernández-Suárez et al., 2008). First, BirA was fused to p33 for targeting to the replication site, whereas AviTag was fused to Atg11 to monitor proximity to p33 in yeast cells. We co-expressed BirA-p33 and Avi-Atg11 in yeast under low biotin condition, followed by a brief biotin pulse (Fig. 4C). This led to biotinylation of Avi-Atg11 in yeast (Fig. 4C, lanes 1–2), indicating the close proximity of p33 replication protein and Atg11 in yeast cells. In addition, streptavidin-based capturing of biotinylated proteins also resulted in the recovery of the biotinylated Avi-Atg11 from yeast expressing BirA-p33 (Fig. 4C, second panel). Avi-Atg11 was not biotinylated when His_6-p33 was expressed as a control, suggesting that yeast does not have nonspecific biotin-ligase activity on Avi-Atg11 (Fig. 4C, lanes 3–4).

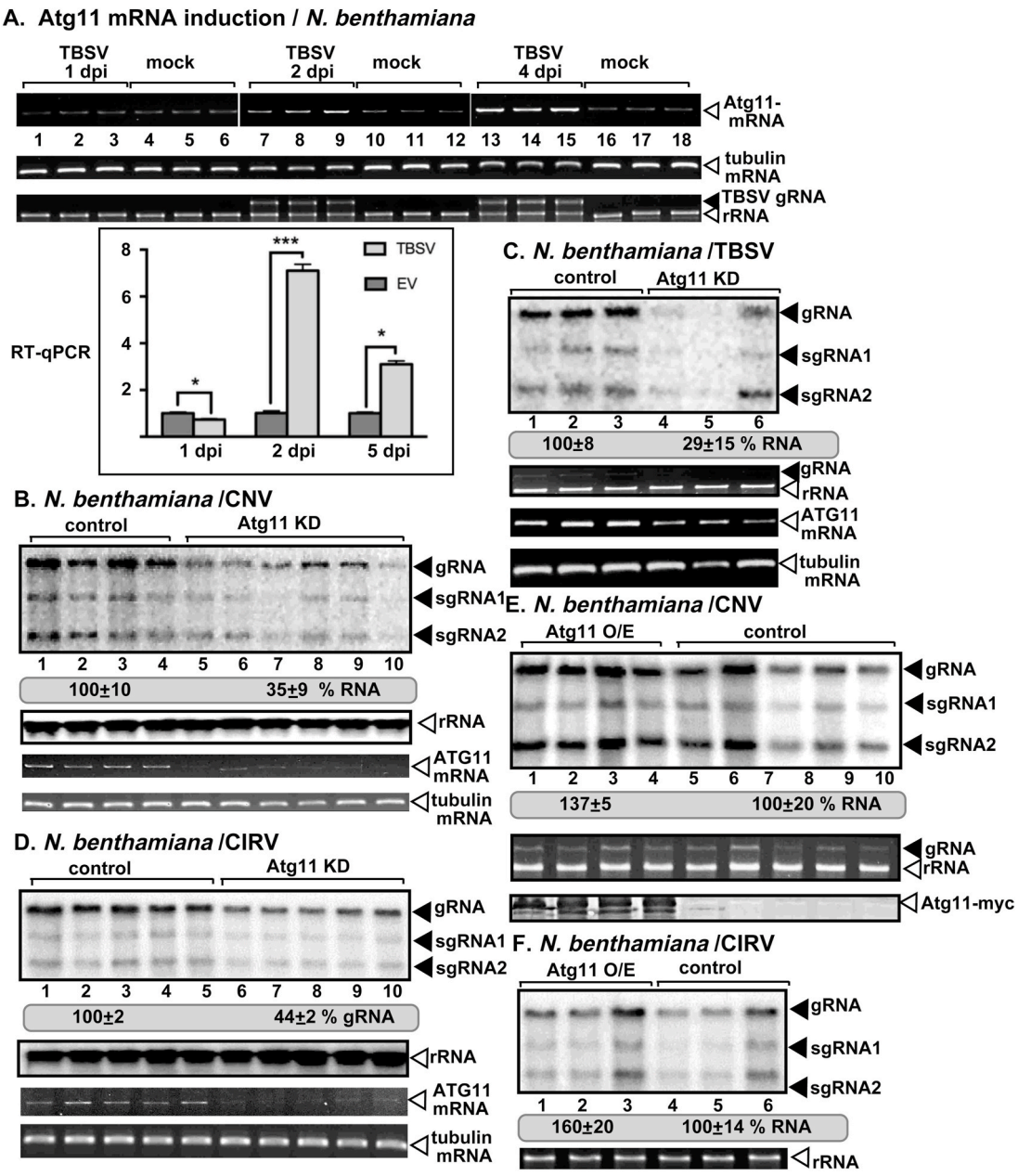

Fig. 2. The effect of Atg11 on tombusvirus replication in *N. benthamiana* plants. (A) Top panel: Induction of Atg11 mRNA expression in the inoculated leaves (1 and 2 dpi, respectively) or systemically-infected leaves (4 dpi) of *N. benthamiana* plants infected with TBSV was detected by semi-quantitative RT-PCR. Middle panel: RT-PCR of tubulin mRNA was used as a control. Middle panel: Ribosomal RNA is shown as a loading control in an ethidium-bromide stained agarose gel. Note that the TBSV gRNA is also visible in this gel. Bottom panel: Graph: Real time RT-qPCR analysis of Atg11 mRNA levels in the agroinfiltrated leaves (1 and 2 dpi, respectively) or systemically-infected leaves (5 dpi) of *N. benthamiana* plants agroinfiltrated with pCAM-TBSV or pGD empty vectors as control. (B–D) Top panel: The accumulation of the CNV, TBSV and CIRV genomic (g)RNA in Atg11-silenced (Atg11 KD) *N. benthamiana* plants 2.5, 2 and 3 dpi, respectively, in the inoculated leaves was measured by northern blot analysis. Agroinfiltration of pGD-CNV^{20Kstop} or sap inoculation with TBSV and CIRV was done 10 days after silencing of Atg11 expression. Agroinfiltration of tobacco rattle virus (TRV) vector carrying NbAtg11-R2+R3 or 3′-terminal GFP (as a control) sequences was used to induce VIGS. Second panel: Ribosomal RNA is shown as a loading control in a northern blot or in an ethidium-bromide stained agarose gel. Third panel: RT-PCR analysis of NbAtg11 mRNA level in the silenced and control plants. Fourth panel: RT-PCR analysis of tubulin mRNA level in the silenced and control plants. Each experiment was repeated three times. (E–F) Overexpression of Atg11 stimulates CNV and CIRV gRNA accumulation in *N. benthamiana* plants.

Second, we expressed BirA-tagged p33 replication protein in *N. benthamiana*, which led to biotinylation of Avi-tagged NbAtg11 (Fig. 4D, lanes 1–2). The Avi-tagging of Atg11 was necessary to detect the biotinylated Atg11 in the presence of p33-His$_6$-BirA in *N. benthamiana* (Fig. 4D, lanes 3–4, see also Fig. S3B). Third, in a reciprocal setting, co-expression of BirA-tagged NbAtg11 resulted in the biotinylation of Avi-tagged p33 in *N. benthamiana* (Fig. 4E, lanes 1–2). In the absence of the BirA fusion, expression of Atg11 did not lead to biotinylation of Avi-tagged p33 in *N. benthamiana* (Fig. 4E, lane 3). Altogether, the above data confirm the close proximity of Atg11 host protein and the tombusvirus p33 replication protein in yeast and plant cells.

To provide additional evidence that the plant Atg11 is recruited into VROs through the interactions with the TBSV p33 or CIRV p36 replication proteins, we have conducted bimolecular fluorescence complementation (BiFC) experiments in *N. benthamiana* leaves. The BiFC

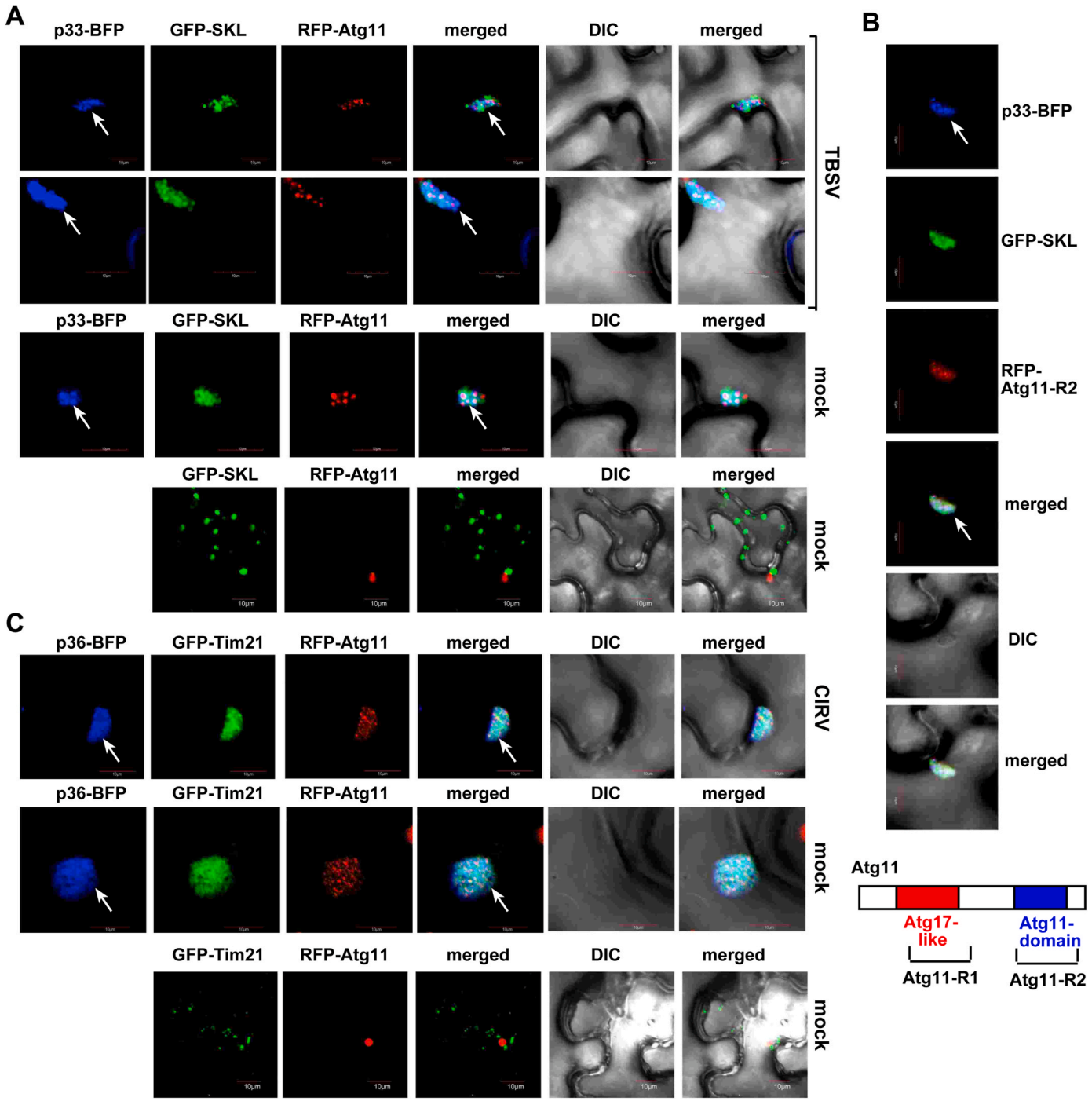

Fig. 3. Recruitment of Atg11 by the TBSV p33 and the CIRV p36 replication proteins into VROs in *N. benthamiana*. (A) Confocal microscopy images show efficient co-localization of TBSV p33-BFP replication protein and the RFP-Atg11 within VROs consisting of clustered peroxisomes, marked by GFP-SKL peroxisomal matrix marker in *N. benthamiana* leaves. Expression of these proteins from the 35S promoter was done after co-agroinfiltration into *N. benthamiana* leaves. The plant leaves were either TBSV-infected or mock-inoculated as shown. Scale bars represent 10 μm. (B) Co-localization of the R2 domain of Atg11 with TBSV p33 in plant cells. See further details in panel A. (C) Confocal microscopy images show efficient co-localization of CIRV p36-BFP replication protein and the RFP-Atg11 within VROs consisting of clustered mitochondria, marked by GFP-AtTim21 mitochondrial marker in *N. benthamiana* leaves. See further details in panel A. Scale bars represent 10 μm. Each experiment was repeated.

signals revealed specific interactions between Atg11 and the TBSV p33 and p92^{pol} replication proteins within the VROs (Fig. 5A, also, see the bottom panel for the negative control experiment). Furthermore, we tested the interaction between the C-terminal Atg11-like and the N-proximal Atg17-like domains (see Fig. 3B) of the full-length NbAtg11 and the replication proteins via BiFC. Both domains were involved in the interaction and recruitment of Atg11 by the TBSV replication proteins into VROs, albeit the Atg11-like domain interaction with p33 and p92^{pol} was more pronounced than Atg17-like domain in these experiments (Fig. 5B). Interestingly, the CIRV p36 replication protein showed similar interaction with Atg11 and its two domains within the VROs (Fig. 5C). Thus, most of the interactions between Atg11 and the tombusviral replication proteins take place within the VROs in *N. benthamiana*.

Co-purification of co-opted vMCS proteins with the TBSV

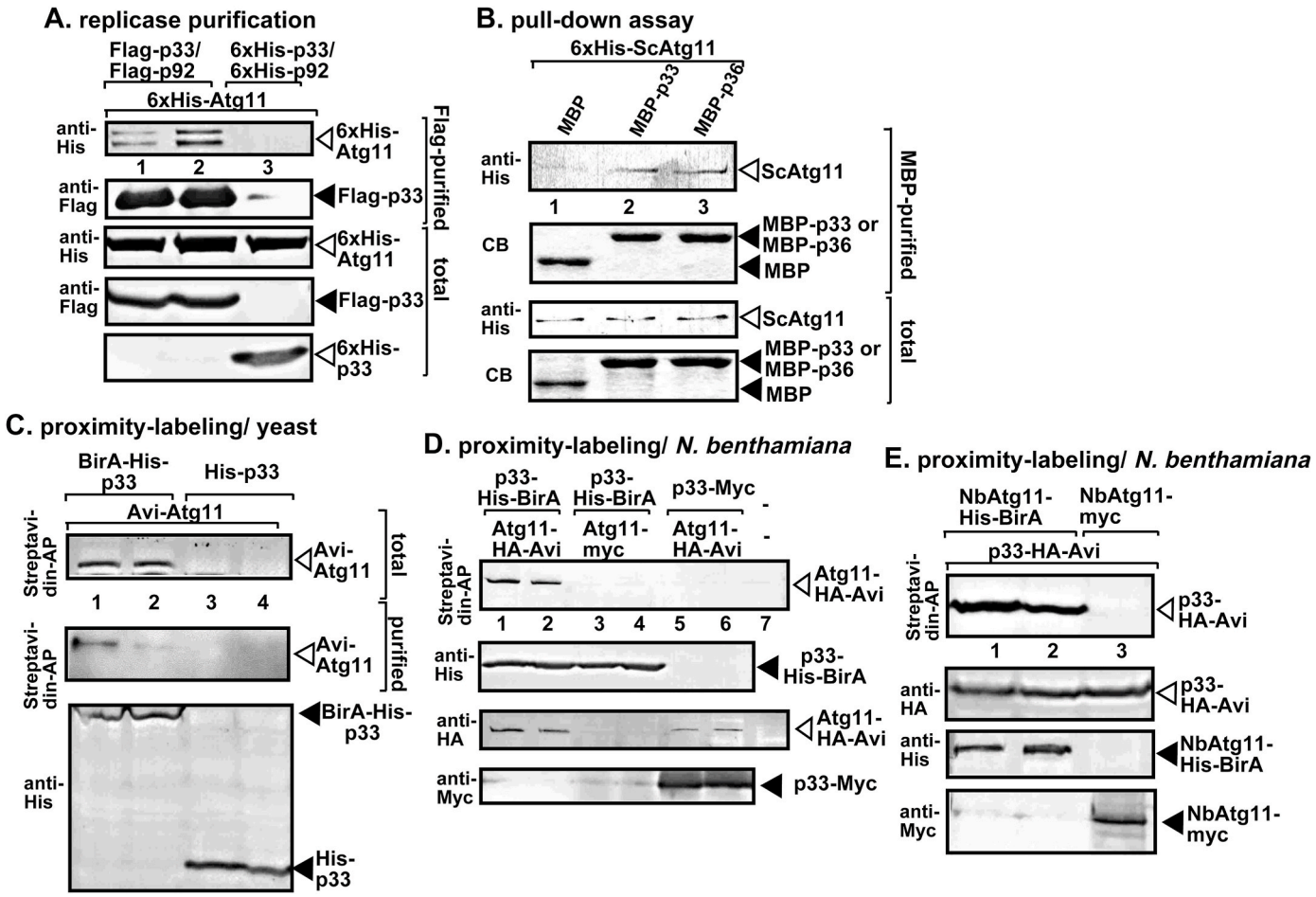

Fig. 4. Interaction between tombusvirus replication proteins and Atg11. (A) Co-purification of the yeast His_6-Atg11 with TBSV Flag-p33 and Flag-$p92^{pol}$ replication proteins from detergent-solubilized subcellular membranes. Top two panels: western blot analysis of co-purified His_6-Atg11 (lanes 1–2) with Flag-affinity purified Flag-p33 and Flag-$p92^{pol}$. His_6-tagged proteins were detected with anti-His antibody, while Flag-p33 was detected with anti-Flag antibody. The negative control was from yeast expressing His_6-p33 and His_6-$p92^{pol}$ purified in a Flag-affinity column (lane 3). Samples were cross-linked with formaldehyde. Bottom two panels: western blot of total His_6-Atg11 and Flag-p33 in the total yeast extracts. (B) Pull-down assay including the yeast GST-His_6-Atg11 and either the MBP-tagged TBSV p33 or CIRV p36 replication proteins. Note that we used the soluble C-terminal region of TBSV p33 or CIRV p36 replication proteins, which lacked the N-terminal *trans*-membrane domain. Top panel: western blot analysis of the captured yeast GST-His_6-Atg11 with the MBP-affinity purified p33/p36 was performed with anti-His antibody. The negative control was the MBP (lane 1). Middle panel: Coomassie-blue stained SDS-PAGE of the captured MBP-p33, MBP-p36 and MBP. Bottom panels: western blot analysis of GST-His_6-Atg11 in total extracts. Coomassie-blue stained SDS-PAGE of the MBP-p33, MBP-p36 and MBP in total extracts. Each experiment was repeated three times. (C) Protein proximity-labeling with biotin in yeast. P33 replication protein was fused to BirA biotin ligase, whereas Atg11 was fused to Avi-tag. Biotin treatment lasted for 2h. Top image shows the western blot analysis of the biotinylated Avi-Atg11 in total protein extract, whereas the second image shows the streptavidin-based purified biotinylated Avi-Atg11. Biotinylated Avi-Atg11 was detected with streptavidin-conjugated AP. Bottom image shows western blot analysis of BirA-His_6-p33 in total protein extracts. Yeast expressing His_6-p33 and Avi-Atg11 was used as a negative control. (D) Protein proximity-labeling with biotin in *N. benthamiana*. Agroinfiltration was used to express p33 replication protein, which was fused to BirA biotin ligase, and Atg11-Avi-tag. Biotin treatment lasted for 40 min. Top image shows the western blot analysis of the biotinylated Atg11-Avi detected with streptavidin-conjugated AP in total protein extracts. See further details in panel C. (E) Reciprocal protein proximity-labeling with biotin in *N. benthamiana*. Agroinfiltration was used to express Atg11-His_6-BirA, and p33-HA-Avi-tag replication protein. See further details in panel D.

replicase is affected by ATG11 deletion in yeast. Although the canonical function of Atg11 is based on its scaffold function during the selective autophagy process (Eickhorst et al., 2020; Zientara-Rytter and Subramani, 2020), we hypothesized that tombusviruses might be able to exploit the tethering function of Atg11 during replication. Our model is based on the documented interaction of Atg11 with Fis1 mitochondrial fission protein, which is involved in virus-induced membrane contact site (vMCSs) formation (Lin et al., 2021). TBSV induces the formation of vMCSs between the ER membrane and the peroxisomal membrane to facilitate transfer of lipids, sterols and PI(4)P phosphoinositide within VROs (Barajas et al., 2014b; Nagy et al., 2016; Sasvari et al., 2018, 2020).

To test the putative role of Atg11 in vMCS formation, first we measured the amount of co-purified VAP (VAMP-associated protein), namely the yeast ER-resident Scs2 VAP protein, which is a tethering protein required for vMCS formation (Barajas et al., 2014b). We purified the tombusvirus replicase from membrane fraction derived from atg11Δ and WT yeasts, followed by measuring the co-purified His_6-Scs2 by western blotting. In comparison with the replicase preparations from WT yeast, the replicase preparations from atg11Δ yeast contained less Scs2 VAP (Fig. 6A, compare lanes 1–2 and 3–4). These observations suggest that recruitment of Scs2 VAP protein to the viral replication compartment, likely to vMCSs, is affected by Atg11.

Another vMCS protein is Osh6 oxystrerol-binding protein, which must be recruited from the cytosol to vMCSs via protein-protein interactions (Barajas et al., 2014b). In comparison with the replicase preparations from WT yeast, the replicase preparations from atg11Δ yeast contained ~5-times less Osh6 (Fig. 6B, compare lanes 1–2 and

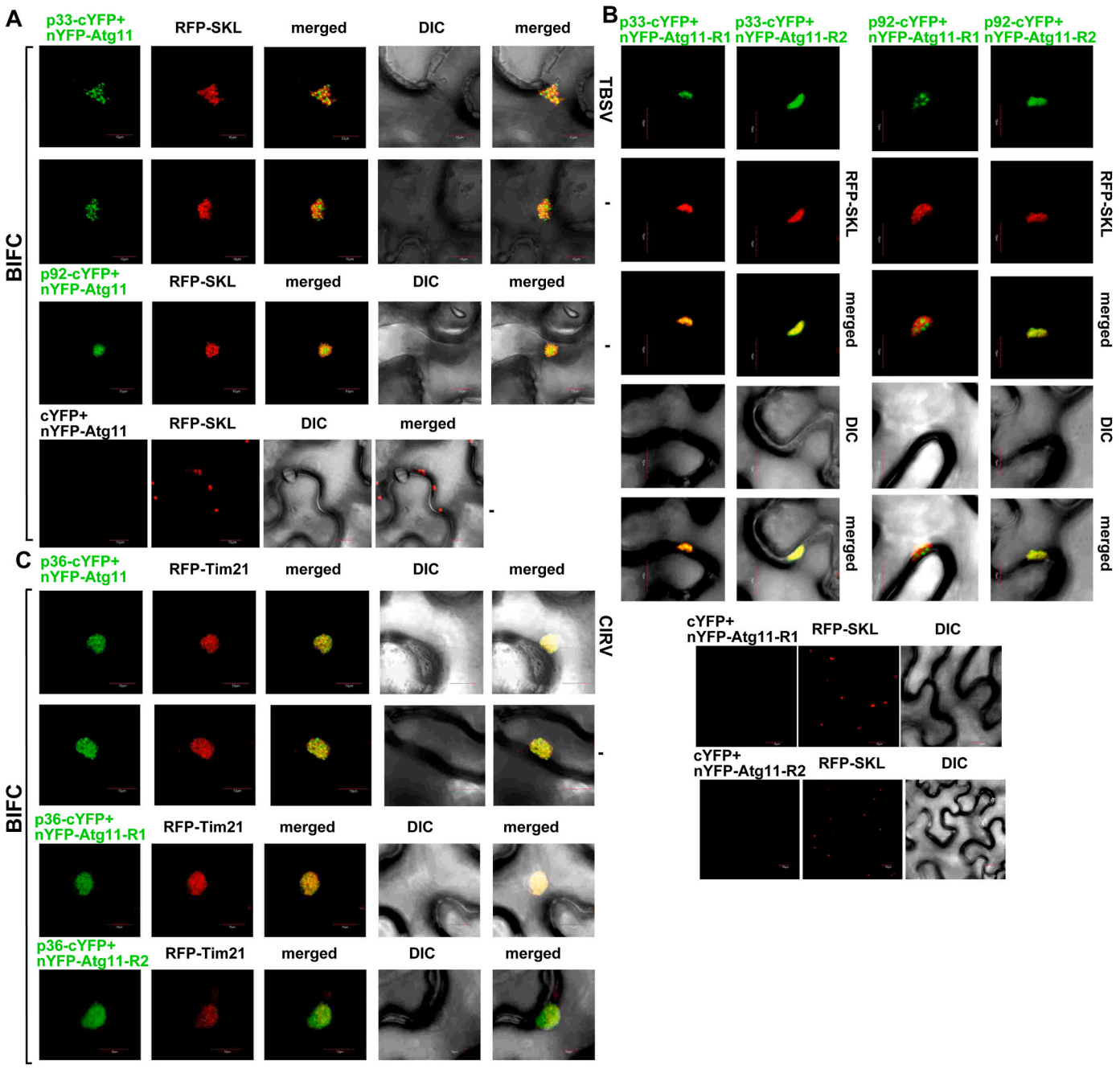

Fig. 5. BiFC studies of the interaction between Atg11 and replication proteins within VROs in *N. benthamiana*. (A) Top two panels: Interaction between TBSV p33-cYFP replication protein and the nYFP-Atg11 protein was detected by BiFC. The merged images show the efficient co-localization of RFP-SKL with the BiFC signal, indicating that the interaction between p33 replication protein and Atg11 occurs in VROs in clustered peroxisomal membranes. Third panel: Interaction between TBSV p92-cYFP replication protein and the nYFP-Atg11 protein was detected by BiFC. Bottom panel: negative BiFC control. (B) Interaction between TBSV p33-cYFP or p92-cYFP replication proteins and the R1 (Atg17-like) or R2 (Atg11-like) domains of Atg11 proteins were detected by BiFC. See further details in panel A. (C) Interactions between CIRV p36-cYFP replication protein and the nYFP-Atg11 protein or the R1 or R2 domains of Atg11 were detected by BiFC. The merged images show the efficient co-localization of RFP-AtTim21 with the BiFC signal, indicating that the interaction between p36 replication protein and Atg11 occurs in VROs consisting of aggregated mitochondria. See further details in panel A. Scale bars represent 10 μm. Each experiment was repeated three times.

3–4). Thus, Atg11 affects the recruitment of Osh6 protein to vMCSs.

The third vMCS host protein tested was Fis1 mitochondria/peroxisome fission protein, which serves as a tether in the acceptor membrane (i.e, peroxisome) during vMCS formation (Lin et al., 2021). The replicase preparations from atg11Δ yeast contained similar amounts of Fis1 protein as in the replicase preparations from WT yeast (Fig. 6C, compare lanes 1–2 and 3–4). Thus, Fis1 recruitment by p33 into vMCS does not depend on the co-opted Atg11 protein. This Atg11 independency might be due to binding of p33 to the mitochondrial/peroxisomal Fis1 prior to recruitment of the cytosolic Atg11 into vMCS.

The fourth vMCS protein studied here was the ER-resident Sac1 PI4P phosphatase, which forms a protein interaction hub with the syntaxin18-like Ufe1 SNARE protein in the ER to help formation of vMCS by the p33 replication protein (Sasvari et al., 2018, 2020). Interestingly, the replicase preparations from atg11Δ yeast contained ~6-times less amounts of Sac1 protein than present in the replicase preparations from WT yeast (Fig. 6D, compare lanes 1–2 and 3–4). These data suggest that in the absence of Atg11, vMCS formation is likely less

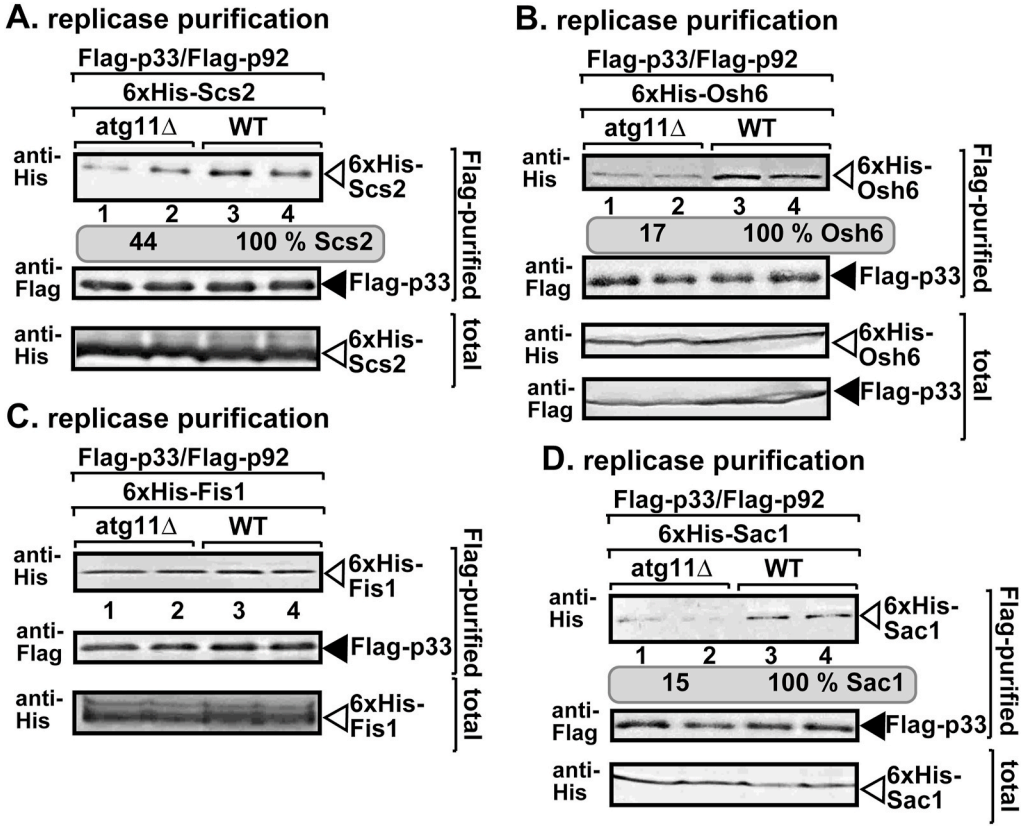

Fig. 6. Atg11 facilitates the recruitment of the cellular ER-resident VAP protein, Sac1 and Osh6 proteins into tombusvirus replication compartment. (A) Co-purification of the yeast His_6-Scs2 VAP protein with TBSV Flag-p33 and Flag-$p92^{pol}$ replication proteins from subcellular membranes of WT or atg11Δ yeast strains. Top two panels: western blot analysis of co-purified His_6-Scs2 detected with anti-His antibody, whereas Flag-p33 was detected with anti-Flag antibody. Samples were cross-linked with formaldehyde. Bottom panel: western blot of total His_6-Scs2 in the total yeast extracts. (B) Co-purification of the yeast His_6-Osh6 with TBSV Flag-p33 and Flag-$p92^{pol}$ replication proteins from subcellular membranes of WT or atg11Δ yeast strains. See further details in panel A. (C) Co-purification of the yeast His_6-Fis1 with TBSV Flag-p33 and Flag-$p92^{pol}$ replication proteins from subcellular membranes of WT or atg11Δ yeast strains. See further details in panel A. (D) Co-purification of the yeast His_6-Sac1 with TBSV Flag-p33 and Flag-$p92^{pol}$ replication proteins from subcellular membranes of WT or atg11Δ yeast strains. See further details in panel A. Each experiment was repeated.

efficient. In addition, Atg11 likely participates in the early steps of vMCS formation, which also depends on Sac1 and Fis1 (Lin et al., 2021; Sasvari et al., 2020).

Co-localization and protein proximity-labeling of Atg11 and vMCS proteins. First, we performed BiFC experiments with Atg11 and Sac1 vMCS protein in plants. Interestingly, we found that the interaction between Atg11 and Sac1 takes place within a limited portion of the large VROs induced by the TBSV p33 replication protein in *N. benthamiana* (Fig. 7A). Similar picture was obtained for the interaction between Atg11 and Sac1 in VROs induced by the CIRV p36 replication protein (Fig. 7B). These data strongly indicate that Atg11 interacts with Sac1 vMCS protein within VROs of tombusviruses. We noted that Atg11 also interacts with Sac1 in the absence of tombusvirus infections in plant cells, albeit the interaction does not take place in the peroxisomal membranes (marked by RFP-SKL, Fig. 7A).

We also used BirA-Atg11-based expression to show that the vMCS proteins Osh6, Scs2 VAP and Sac1 lipid phosphatase, which were individually Avi-tagged, were biotin-labeled in yeast (Fig. 8). The expression of p33 replication protein did not influence the extent of the above proximity-labeling. BirA-p33 expression also showed that the vMCS proteins (Avi-Osh6, Avi-Scs2, Avi-Fis1 and Avi-Sac1) were biotin-labeled in yeast (Fig. 8B–C), whereas eEF1A (Avi-Tef1) translation elongation factor, which strongly interacts with the p92 RdRp and the TBSV (+)RNA (Li et al., 2008, 2009, 2010), was not biotin-labeled (Fig. S4). Expression of Atg11-BirA in *N. benthamiana* infected with CNV or mock-inoculated led to the biotin-labeling of the Avi-tagged PVA12 VAP and ORP3 oxysterol-binding protein (co-opted members of vMCS) (Fig. 8D). Based on these data, we suggest that Atg11 is localized in close proximity of the known vMCS proteins in yeast and plants. This supports that Atg11 is part of the tombusvirus-induced vMCS.

Atg11 contributes to vMCS functions. First, we tested the major function of the virus-induced vMCSs, which is to facilitate the enrichment of sterols within internal compartments (Barajas et al., 2014b), in the absence of *ATG11* in yeast. The re-distribution of ergosterols (the sterol component in yeast) in yeast cells was monitored with filipin dye using fluorescent microscopy (Beh et al., 2001). As documented previously (Barajas et al., 2014b; Lin et al., 2021; Sasvari et al., 2020), we found that TBSV replication resulted in redistribution of ergosterol mostly from the plasma membrane to internal locations into punctate structures (Fig. 9). However, *ATG11* deletion in yeast greatly reduced the internal ergosterols in the presence of the TBSV components, based on the much smaller-sized and dimmer lipid puncta than those observed in WT yeast (Fig. 9). We calculated ~4 times less number of yeast cells containing large internal puncta (filling 20% or more of the cell volume) in case of atg11Δ versus WT yeasts replicating TBSV (Fig. 9). Ergosterol redistribution in atg11Δ yeast was comparable to the ergosterol localization in fis1Δ yeast replicating TBSV (Fig. 9) as we documented before (Lin et al., 2021). Fis1 mitochondrial fission protein acts as a co-opted tethering protein during vMCS formation (Lin et al., 2021). Expression of Atg11 from a plasmid in atg11Δ yeast replicating TBSV led to efficient redistribution of ergosterol to internal locations, comparable to those observed in WT yeast (Fig. 9). *ATG11* deletion in yeast caused some changes in ergosterol distribution, resulting in ergosterol accumulation in both the plasma membrane and in small punctate structures in the absence of the viral components (Fig. 9). These ergosterol-containing punctate structures were frequently associated with the plasma membrane. Overall, ergosterol distribution in atg11Δ yeast was mostly comparable with that seen in WT yeast in the absence of the viral components (Fig. 9). These data suggest that the co-opted Atg11 is involved in ergosterol enrichment, likely within vMCSs induced by p33 replication protein in yeasts.

The second approach was based on the previous observation (Lin et al., 2021) that different co-opted tethering proteins within vMCS affect the function of other tethering proteins, thus influencing TBSV replication. For example, over-expression of tethering proteins in yeast can partially complement the inhibitory effect of deletion of a different tethering protein in vMCS on TBSV replication (Lin et al., 2021).

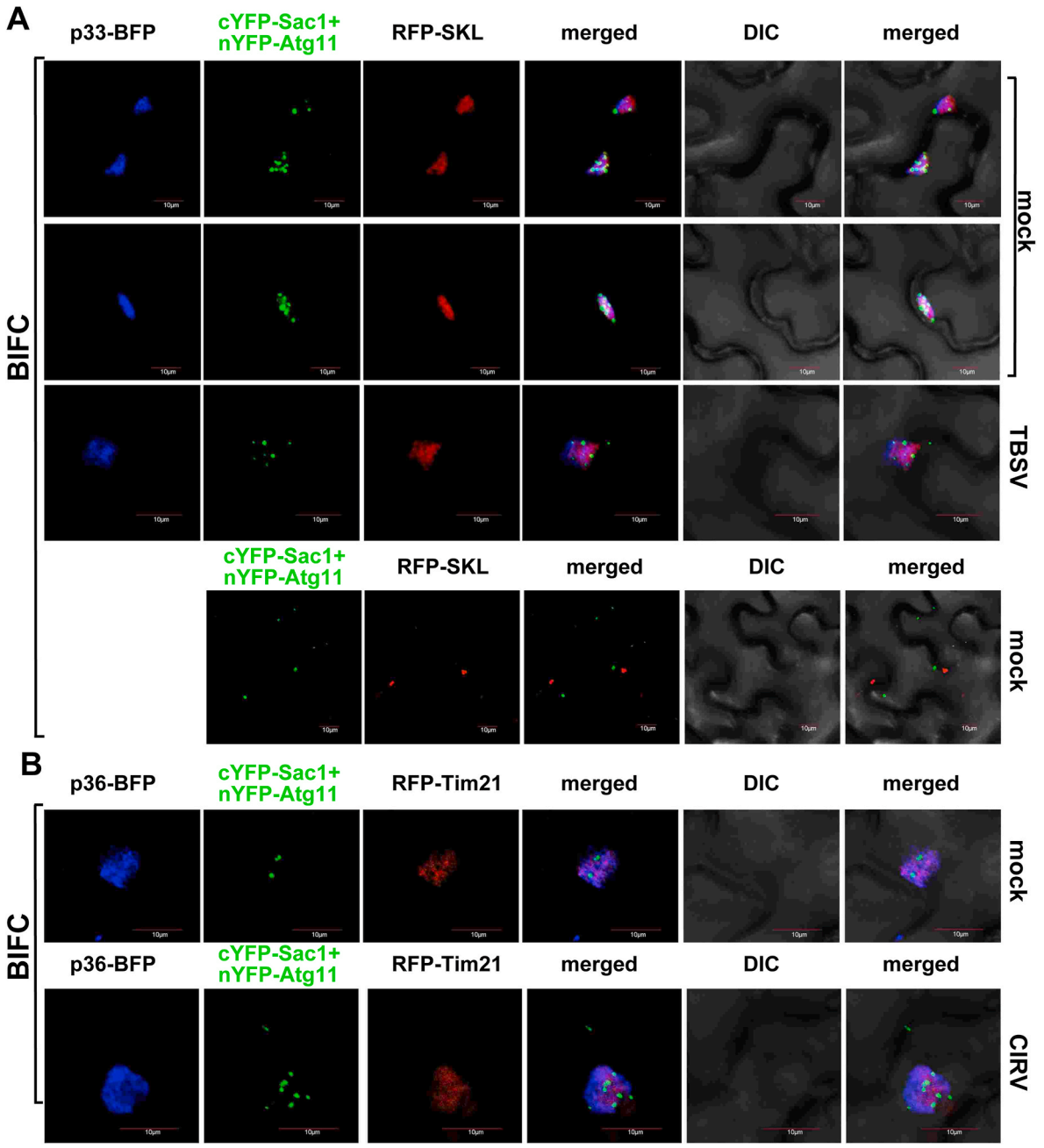

Fig. 7. Interaction between Atg11 and Sac1 PI4P phosphatase protein within VROs in *N. benthamiana*. (A) BiFC approach was used to demonstrate interaction between nYFP-Atg11 and cYFP-Sac1 proteins within the TBSV p33-BFP-positive VROs (B) or CIRV p36-BFP-positive VROs. Expression of the above proteins from 35S promoter was done after co-agroinfiltration into *N. benthamiana* leaves infected with either TBSV or CIRV or mock-inoculated. Scale bars represent 10 μm. Each experiment was repeated.

Therefore, we made a double-deletion yeast strain missing *ATG11* and *FIS1*. TBSV replication was decreased to ~half level in atg11Δ/fis1Δ yeast strain when compared to the replication level in single deletion atg11Δ or fis1Δ yeast strains (Fig. 10A, lanes 8–10). The accumulation level of p33 was further reduced in the double-deletion yeast strain as well, indicating reduced stability of p33 under these conditions, likely due to reduced sterol enrichment at vMCS in atg11Δ/fis1Δ yeast strain (Xu and Nagy, 2017).

Over-expression of Sac1 PI4P phosphatase, which is a co-opted vMCS protein with tethering function as well (Lin et al., 2021; Sasvari et al., 2020) in atg11Δ yeast led to partial recovery of TBSV repRNA accumulation (Fig. 10B, lanes 4–6 versus 1–3). Therefore, we suggest that when Sac1 is abundant in cells, then Sac1 could easily be recruited by the tombusvirus replication proteins even in the absence of Atg11. These data suggest that Sac1 scaffold function partially complements the putative tethering function of Atg11 at vMCS, but only when Sac1 is abundant due to over-expression.

Over-expression of Sac1 in the double-deletion (atg11Δ/fis1Δ) yeast strain only resulted in partial complementation of TBSV replication (Fig. 10B, lanes 10–12 versus 7–9). TBSV replication was very low under this condition, suggesting that the lack of two tethering proteins (i.e., Atg11 and Fis1) cannot be compensated by over-expression of a single Sac1 scaffold protein to fully support TBSV replication, likely due to incomplete vMCS functions. Nevertheless, the single deletion yeast strains showed that the expression of all these co-opted tethering proteins is needed to support robust TBSV replication, as observed in WT

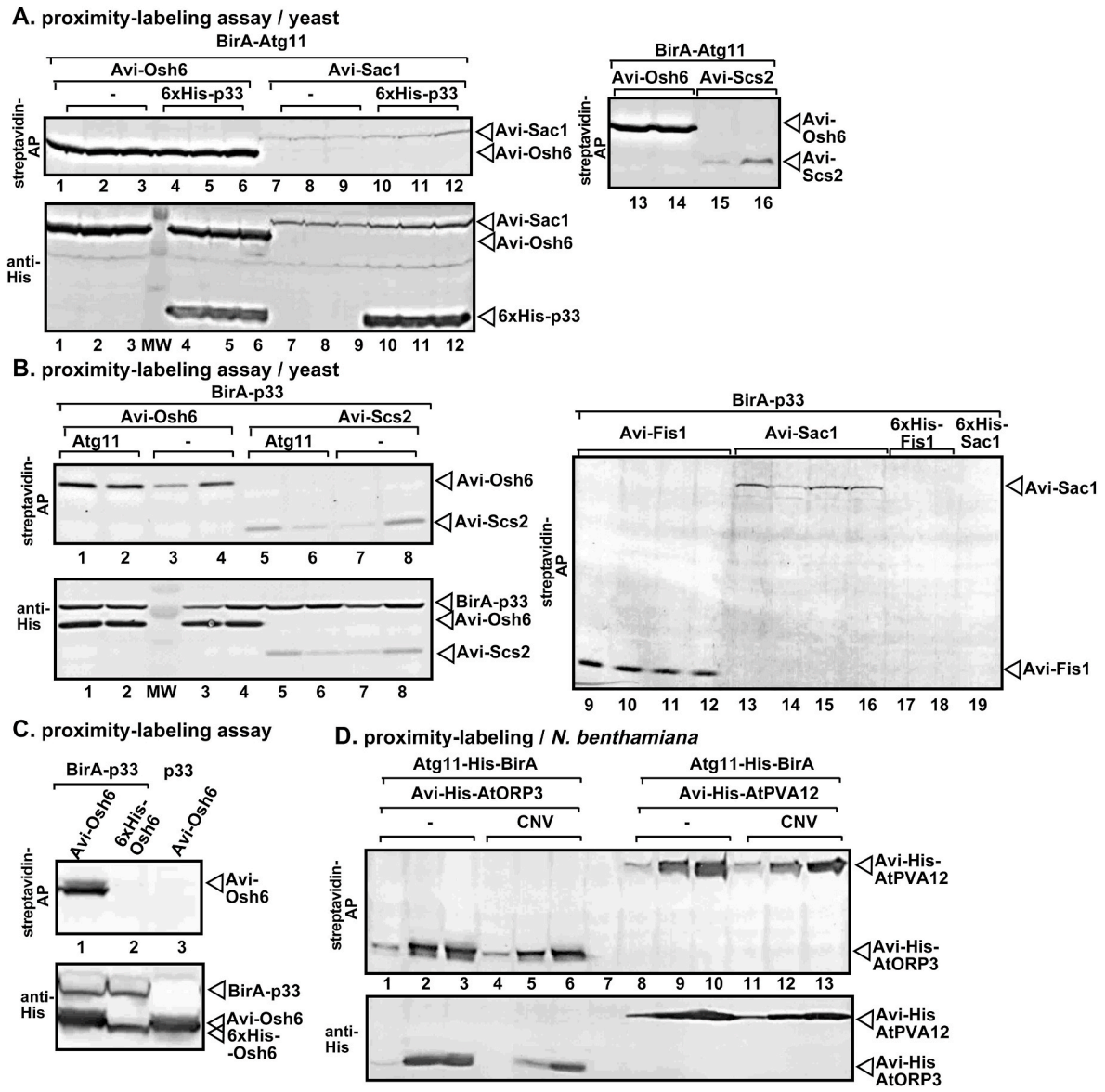

Fig. 8. Protein proximity-labeling of vMCS proteins with biotin in yeast and plants. (A) Proximity labeling with BirA-Atg11 of the Avi-tagged Osh6, Sac1 and Scs2 vMCS proteins. His_6-p33 was co-expressed in the marked samples. Biotin treatment lasted for 30 min. Top image shows the western blot analysis of the biotinylated Avi-tagged proteins detected with streptavidin-conjugated AP in total protein extracts. Bottom image shows western blot analysis of vMCS proteins via anti-His antibody in total protein extracts. (B) Proximity labeling with BirA-p33 of Avi-tagged Osh6, Scs2 Fis1 and Sac1 vMCS proteins. Atg11 was co-expressed in the marked samples. Biotin treatment lasted for 30 min. Top image shows the western blot analysis of the biotinylated Avi-tagged proteins detected with streptavidin-conjugated AP in total protein extracts. Bottom image shows western blot analysis of vMCS proteins via anti-His antibody in total protein extracts. (C) Control experiment for proximity labeling with BirA-p33 of Avi-Osh6. See panel B for further details. (D) Proximity labeling with Atg11-BirA of the Avi-tagged ORP3 oxysterol-binding protein and PVA12 VAP protein, which are core vMCS proteins. The time points were 31 h (lanes 1, 4, 8 and 11); 48 h (lanes 2, 5, 9 and 12); and 56 h (lanes 3, 6, 10 and 13) after agroinfiltration. Biotin treatment lasted for 60 min. Plants were infected with CNV or not-infected as shown. Top image shows the western blot analysis of the biotinylated Avi-tagged proteins detected with streptavidin-conjugated AP in total protein extracts. Bottom image shows western blot analysis of vMCS proteins via anti-His antibody in total protein extracts.

yeast. This is likely due to the limited accessibility of these proteins in yeast, thus "forcing" tombusviruses to compete with normal cellular processes to subvert the host factors for pro-viral functions within vMCS.

Tombusvirus VROs become RNAi-sensitive in the absence of Atg11 autophagy protein in yeast. The VROs formed in WT yeast or in plants provide protection against antiviral responses, including RNAi (Barajas et al., 2014a; Kovalev et al., 2017; Lin et al., 2021; Sasvari et al., 2020). The ability of VROs to protect the viral RNA can be tested using the reconstituted RNAi machinery from *S. castellii* with the two-component *DCR1* and *AGO1* genes (Drinnenberg et al., 2009; Kovalev et al., 2017). This approach allows for the probing of the contribution of individual co-opted host factors to the protection of the viral RNAs (Kovalev et al., 2017; Lin et al., 2021). We expressed the reconstituted RNAi machinery in atg11Δ yeast replicating TBSV repRNA and compared it with the RNA protection provided in fis1Δ and WT yeasts. Interestingly, deletion of *ATG11* gene in yeast led to poor protection of the TBSV RNA (Fig. 11). The ~50% reduction of repRNA in atg11Δ expressing the RNAi components was comparable with that observed in fis1Δ yeast strain (Lin et al., 2021), but less than that found in WT yeast (Fig. 11). As previously found, VROs formed in WT yeast protected the viral RNAs against the RNAi machinery (Fig. 11) (Feng et al., 2020; Kovalev et al., 2017). Based on these data, we suggest that similar to Fis1, Atg11 is also needed for the biogenesis of the protective VROs against the antiviral RNAi machinery.

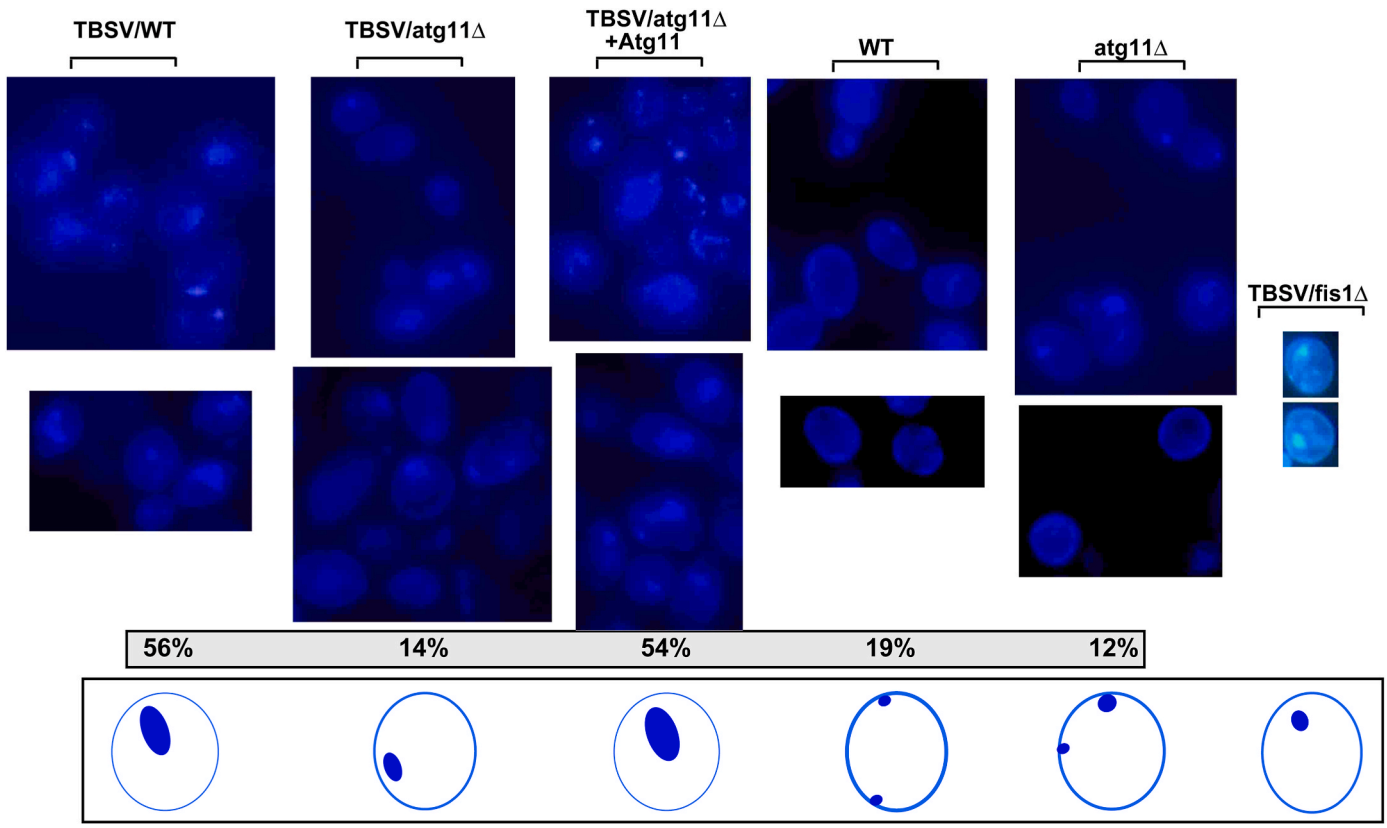

Fig. 9. Atg11 affects sterol re-localization to internal sites in yeast replicating TBSV RNA. Fluorescent microscopic images of yeast cells stained with the filipin dye. Decreased level of re-localization of ergosterols to internal punctate structures in atg11Δ yeast replicating TBSV (second row from left) in comparison with WT yeast (first row from left) or atg11Δ yeast expressing Atg11 from a plasmid (third row from left). Yeasts expressed the p33 and p92 replication proteins and the TBSV repRNA. We also show the previously characterized effect of Fis1 deletion on sterol distribution in fis1Δ yeast replicating TBSV, which results in reduced ergosterol re-distribution from the plasma membrane to internal punctate structures, similar to that observed in atg11Δ yeast. The control fluorescent microscopic images of yeast cells lacking viral components are shown in the panels on the right. Note that filipin stains ergosterols present mostly in the plasma membrane in virus-free WT or atg11Δ yeast cells. We calculated the percentage of yeast cells, which represented ergosterol-rich membranes filling 20% or more of the intracellular space in yeast versus minimal or no intracellular puncta. We have based our calculations on total of ~100 or more yeast cells for each experiment. The bottom panel illustrates the representative size and distribution of sterol-rich punctate structures and the plasma membrane. Each experiment was repeated.

3. Discussion

A surprising novel role of Atg11 autophagy-related protein in the formation of vMCS to support **tombusvirus VRO biogenesis.** A major emerging theme in tombusvirus-host interactions is the complexity of the VRO biogenesis, which is central in virus replication (Fernandez de Castro et al., 2017; Molho et al., 2021; Nagy, 2015, 2016; Nagy and Feng, 2021). The viral replication proteins act coordinately together with many co-opted host proteins and subcellular membranes to provide the building blocks, tethers, scaffolds for assembly platforms and enzymatic activities to create VROs (Barajas et al., 2014b; Feng et al., 2019; Inaba et al., 2019; Sasvari et al., 2020; Xu and Nagy, 2016). Tombusviruses only provide the viral RNA, the p33 master regulator and the p92 RdRp to support successful VRO assembly in yeast and plants (Barajas et al., 2014b; Feng et al., 2019; Sasvari et al., 2020; Xu and Nagy, 2016). However, the list of the co-opted host components and the full arsenal of subverted functions they provide for VRO biogenesis is growing, but it is still incomplete. In this paper, we show evidence for a new co-opted host factor, the Atg11 autophagy protein that contributes to VRO biogenesis.

We find that Atg11 interacts with the viral replication proteins *in vitro*, in yeast and plant, which leads to extensive recruitment of Atg11 into VROs in cells. Protein proximity-labeling, BiFC, pull-down assay, and the presence of co-purified Atg11 in the tombusvirus replicase preparations, all suggest direct interaction between Atg11 and the viral replication proteins. Deletion of Atg11 in yeast and Atg11 knockdown in plants has inhibitory effect on the peroxisome-associated TBSV or the mitochondria-associated CIRV replication. Therefore, this study establishes a novel, pro-viral function for the Atg11 autophagy scaffold protein.

The current work shows evidence that Atg11 is involved in the formation of vMCS and the biogenesis of VROs. Accordingly, Atg11 is shown via BiFC to interact with the co-opted Sac1 PI4P phosphatase within VROs in plant cells. In addition, protein proximity-labeling shows the presence of Atg11 in the vicinity of Sac1, Fis1 mitochondrial fission protein, oxysterol transfer protein (Osh6 in yeast) and Scs2 VAP, which are the core proteins involved in vMCS formation within VROs (Barajas et al., 2014a; Lin et al., 2021; Sasvari et al., 2020). Based on TBSV replicase purification experiments, Atg11 affected the recruitment of the core vMCSs-localized proteins, such as the ER-resident VAP protein and Sac1 and the cytosolic Osh6 protein into VROs. On the other hand, we did not find a role for Atg11 in recruitment of the peroxisomal/mitochondrial Fis1 into the tombusvirus replicase. Interestingly, the extent of Atg11 contribution to tombusvirus replication seems to be similar to that observed with Fis1, Sac1, Osh proteins or VAP proteins (Barajas et al., 2014b; Lin et al., 2021; Sasvari et al., 2020). Via inducing vMCS formation, these co-opted host proteins are needed to provide optimal lipid/membrane microenvironment for TBSV replication within VROs. Similar to Atg11, the core vMCS proteins also contribute to p33 stabilization and protection of the viral RNA from degradation by RNAi and other nucleases (Barajas et al., 2014b; Nagy et al., 2016; Sasvari et al., 2020). The p33 replication protein binds to sterols in the

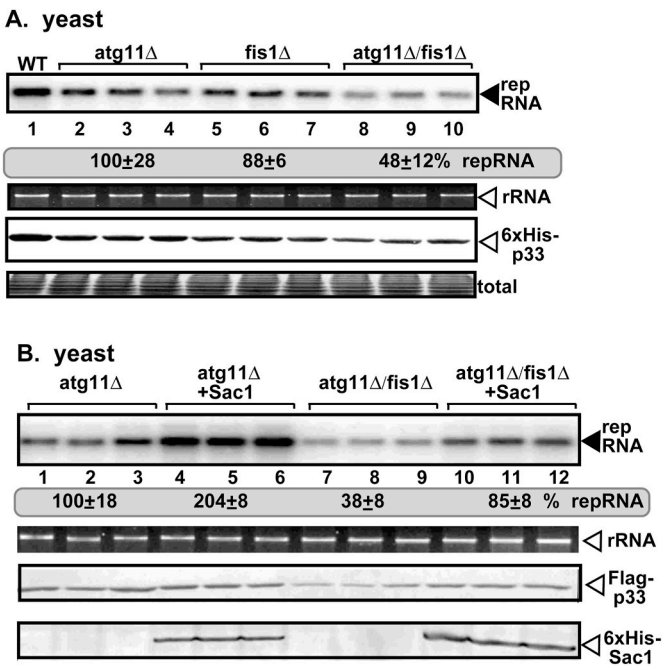

Fig. 10. Double-deletion of *ATG11* and *FIS1* further decreases tombusvirus RNA accumulation in yeast. (A) Replication of the TBSV repRNA was measured by northern blotting 24 h after initiation of TBSV replication in the shown yeast strains. The accumulation level of repRNA was normalized based on the ribosomal (r)RNA. TBSV RNA accumulation in atg11Δ yeast strain was taken as 100% in each experiment. The third panel shows the accumulation of His_6-p33 based on western blotting with anti-His antibody. (B) Complementation of *ATG11* and *FIS1* deletion or double-deletion by over-expression of Sac1 vMCS protein yeast. Northern and western blots with anti-His antibody were done as described in panel A. Each experiment was repeated.

membranes via its CRAC and CARC-like sequences, which are needed to stabilize p33 in yeast or plants (Xu and Nagy, 2017). Therefore, the reduced sterol enrichment in VROs in the absence of one or more of the co-opted vMCS proteins results in reduction in p33 levels. This low level of p33 was also observed in the absence of Atg11 as well (Fig. 1).

Overall, the data obtained with Atg11 support the model that Atg11 contributes to vMCSs formation (Fig. 12). For example, biotin-labeling showed close proximity of p33 and Atg11 to the hijacked core vMCS proteins during tombusvirus replication. Deletion of Atg11 resulted in reduced recruitment of core vMCS proteins by p33. In addition, deletion/depletion of Atg11 has similar inhibitory effects on TBSV replication and protection of the viral RNA from RNAi as depletion of the above vMCSs proteins in yeast and plants. The vMCS structure is unusually stable and abundant (Barajas et al., 2014b; Fernandez de Castro et al., 2017) in comparison with regular, more dynamic MCS structures in healthy cells. These stable vMCS structures are essential for the robust tombusvirus-induced subcellular changes required for rapid and efficient VRO formation, including lipid/sterol enrichment. We propose that the co-opted Atg11, based on its tethering and scaffolding function in selective autophagy (Eickhorst et al., 2020; Zientara-Rytter and Subramani, 2020), also provides comparable tethering and scaffolding function by stabilizing vMCSs within VROs (Fig. 12). Similar picture might be valid for other unrelated human viruses, such as enteroviruses, which also induce and stabilize vMCSs in order to manipulate the lipid composition of the membranes within the viral replication compartment (Laufman et al., 2019; Nagy et al., 2016; van der Schaar et al., 2016). The possible autophagic role of Atg11 in tombusvirus replication will be addressed in subsequent works.

In summary, the roles of increasing number of co-opted host proteins with tethering and scaffolding functions during VRO biogenesis suggest that the tombusviral VRO is an elaborate and complex organelle-like structure. Based on complementation experiments, it seems that the recruitment of the co-opted host tethering proteins, such as Atg11, Fis1, the VAP proteins, Sac1 and Osh6 or ORP3 for viral replication is a rate-limiting step. Nevertheless, tombusviruses need to efficiently recruit the core vMCS proteins to build VRO structures with optimal lipid composition. Moreover, by efficiently recruiting these tethering proteins away from their canonical cellular functions, tombusviruses might affect many cellular processes, which might lead to disease states in infected plants. It will be interesting to learn if other (+)RNA viruses also exploit vMCS and tethering proteins for their replication.

In conclusion, the co-opted Atg11 scaffold protein is required for the formation of membrane contact sites within VROs. This helps tombusviruses to enrich lipids and extend membrane surfaces within VROs, which become ribonuclease-insensitive. The emerging picture is that formation of tombusvirus VROs requires several co-opted tethering and scaffold proteins. Targeting these pro-viral membrane-tethering proteins by inhibitors could open up new antiviral strategies.

4. Materials and methods

Yeast strains and plasmid construction. Plasmids pJW1506 and pJW1234 were obtained from Addgene (Jan et al., 2014). Yeast strain fis1Δ was kindly provided by Dr. Agnes Delahodde (University of Paris-Sud). To create atg11Δ and fis1Δ/atg11Δ yeast strains, the hygromycin resistance gene hphNTI was PCR-amplified from vector pFA6a–hphNT1 (Euroscarf) (Janke et al., 2004) with primers #7890 and primers #7891 and the PCR product was transformed into BY4741 and fis1Δ respectively. Plasmids constructed and primers used in this study are listed in Supplementary Tables S1–4.

Virus RNA replication in yeast. To test repRNA replication, BY4741 (wild type) and atg11Δ, fis1Δ and atg11Δ/fis1Δ yeast strains were transformed with plasmids HpGBK-CUP1-Flagp33/Gal10-DI72,

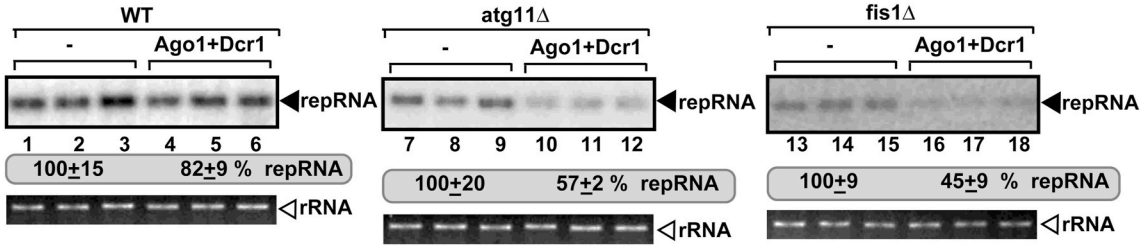

Fig. 11. Deletion of *ATG11* sensitizes tombusvirus RNA to RNAi-based degradation in yeast. Co-expression of *S. castellii* AGO1 and DCR1 in atg11Δ and fis1Δ yeasts reduces TBSV repRNA accumulation to a larger extent than in WT yeast (BY4741). Top panel: Replication of the TBSV repRNA was measured by northern blotting 24 h after initiation of TBSV replication. The accumulation level of repRNA was normalized based on the ribosomal (r)RNA. Note that the TBSV repRNA, p33 and p92 replication proteins were expressed from plasmids. Each sample is obtained from different yeast colonies. Yeast strain not expressing RNAi components is taken as 100% in each experiment. Average value and standard deviation is calculated from all the biological repeats. Ribosomal RNA is shown as a loading control. Each experiment was repeated three times.

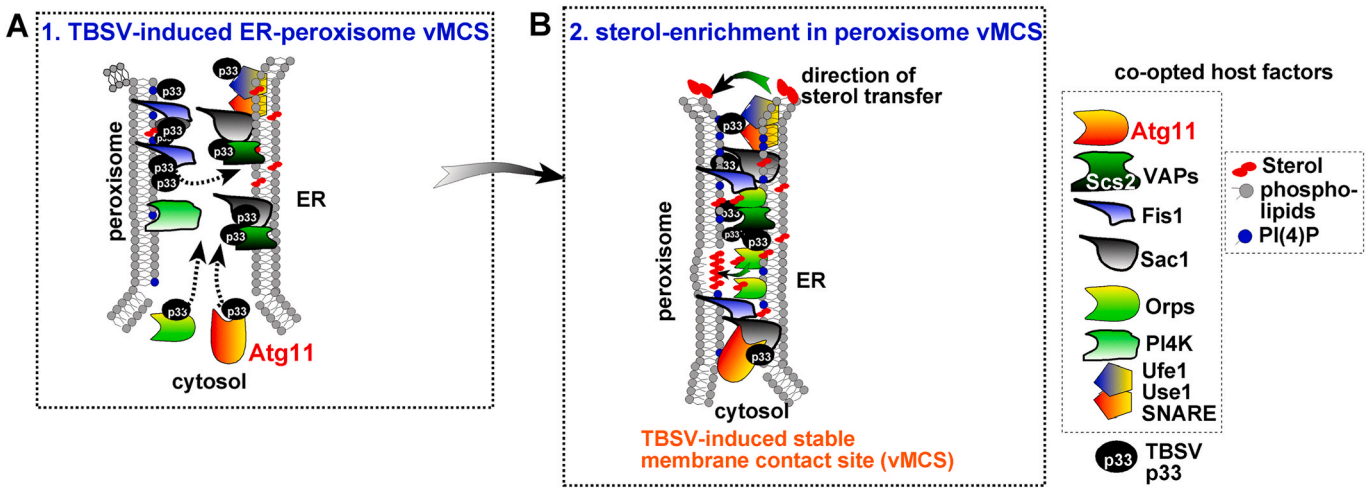

Fig. 12. A model on the functional role of the Atg11 autophagy scaffold protein in the formation of virus-induced vMCS. (A) Expression of the abundant p33 replication protein of TBSV leads to p33 molecules-driven efficient recruitment of Atg11 to vMCS. P33 and Atg11 bind to other vMCS proteins, including the ER-resident VAP tethering protein and Sac1 PI4P phosphatase, the peroxisomal Fis1 mitochondria fission protein and the cytosolic oxysterol-binding proteins (ORP). The cellular PI4K kinase and Ufe1 and Use1 SNARE complex are also recruited into vMCS. We propose that all these interactions lead to the tethering of the peroxisomal membranes to the subdomains of the ER membrane, resulting in the formation and stabilization of vMCSs. (B) The interplay between the co-opted ORP proteins, PI(4)P phosphoinositide and Sac1 facilitates the enrichment of sterols and other lipids within the peroxisomal membranes. These processes render the peroxisomal membranes highly suitable for the formation of VROs needed for virus replication. Please note the related CIRV co-opts similar set of host proteins and builds similar virus-induced vMCS structures utilizing mitochondrial membranes, instead of peroxisomes, and the ER membranes.

LpGAD-CUP1-Flagp92 and UpYES2-NT. To test if plasmid-borne Atg11 expression can rescue virus replication, atg11Δ yeast strain was transformed with HpGBK-CUP1-Flagp33/Gal10-DI72, LpGAD-CUP1-Flagp92 and UpYES2-HisATG11. To test if over-expression of membrane contact sites-associated Sac1 protein can complement tombusvirus replication in atg11Δ yeast strain, wild type BY4741 and atg11Δ yeasts were transformed with HpGBK-CUP1-Flagp33/Gal10-DI72, LpGAD-CUP1-Flagp92 and UpYC-ScSac1. For CIRV replication assay, BY4741 and atg11Δ yeast were co-transformed with plasmids HpESC-CUP1-Flagp36/Gal10-DI72 and LpESC-CUP1-Flagp95 with either UpYES2-NT or UpYES2-HisATG11.

The transformed yeasts were pre-grown in SC-ULH$^-$ (synthetic complete medium without urea, leucine, and histidine) media supplemented with 2% galactose media and 100 μM BCS at 23 °C for 16 h. Then, the yeast cells were cultured in SC-ULH$^-$ media supplemented with 2% galactose and 50 μM $CuSO_4$ at 23 °C for 24 h.

For TBSV replication, yeast strain BY4741 and atg11Δ were transformed with pGBK-Gal-HisT33/Gal-DI72, pGAD-Gal-HisT92 and pYES2-NT. TBSV replication was induced by growing cells at 23 °C in SC-ULH$^-$ medium supplemented with 2% galactose for 24 h at 23 °C.

To test the effect of RNAi on TBSV repRNA accumulation in yeast, we expressed DCR1 and AGO1 proteins (Kovalev et al., 2017). BY4741 and atg11Δ yeast strains were transformed with plasmids HpGBK-CUP1-Hisp33/Gal-DI-72 and LpGAD-CUP1-His92, UpESC-Ura (as a control) or UpESC-Ura-Gal1-HisAgo1-Gal10-HisDcr1. Transformed yeast cells were pre-grown in SC-ULH$^-$ media supplemented with 2% glucose and 100 μM BCS at 29 °C for 16 h. Then, yeasts were cultured in SC-ULH$^-$ media supplemented with 2% galactose and 100 μM BCS at 23 °C for 24 h. Then, the yeast cells were cultured in SC-ULH$^-$ media supplemented with 2% galactose and 50 μM $CuSO_4$ at 23 °C for 16 h. Total RNA and protein extraction and northern-blot and western-blot analyses were done as described (Panavas and Nagy, 2003; Panaviene et al., 2004).

To test the combined functions of Atg11 and other vMCS proteins, we transformed atg11Δ and atg11Δ/fis1Δ yeast strains with HpGBK-CUP1-Flagp33/Gal10-DI72, LpGAD-CUP1-Flagp92 and pYES2-NT or pYES2-Sac1 (Sasvari et al., 2020). Yeast culturing, total RNA extraction and northern-blot analyses were done as described above.

Virus replication in plants. To identify *ATG11* gene sequence in *N. benthamiana*, we used the sequence of *Arabidopsis thaliana ATG11* (AT4G30790) and performed a BLAST search in the QUT Sol101_N. benthamiana_predicted_transcriptome_v101 transcripts database. We find two hits, namely Niben101Scf09742g00014.1 and Niben101Scf02359g00022.1, the coding region of which shares 96.4% identity in amino acid sequence (Supplementary Fig. S1). A chimeric fragment composed of R2 and R3, selected based on highly conserved region within two NbATG11 transcripts, was inserted into TRV2 vector (Bachan and Dinesh-Kumar, 2012) to generate pTRV2-NbATG11-R2+R3 (Supplementary Fig. S2). Agrobacterium C58C1 competent cells were transformed with pTRV2-NbATG11-R2+R3. *N. benthamiana* plants of 4-leaves stage were agroinfiltrated with pTRV1 and pTRV2-NbATG11-R2+R3 or pTRV2-cGFP as a control (OD_{600} 0.5). On the 10th day post agroinfiltration (dpai), upper leaves were agroinfiltrated to express $CNV^{20kstop}$ or inoculated with TBSV or CIRV saps (Jaag and Nagy, 2009). To determine RNA accumulation of TBSV, CNV, and CIRV, the inoculated leaves were collected at 2, 2.5 and 3 dpi, respectively. Total RNA extraction and northern blot analyses were performed as described previously (Jaag and Nagy, 2009). The accumulation of *NbATG11* mRNA and internal reference control *tubulin* mRNA was determined by RT-PCR with primers oligo-d(T) (for RT), #7938 and #7939 for *NbATG11* and #2859 and #2860 for tubulin mRNA (Jaag and Nagy, 2009).

To further test the pro-viral role of Atg11, transient over-expression of Atg11 in *N. benthamiana* leaves was performed by co-agroinfiltration with pGD-ATG11-Myc (OD_{600} 0.6) and pGD-P19 (OD_{600} 0.1). Then the leaves were inoculated with either TBSV or CIRV sap at 16 h post agroinfiltration and the inoculated leaves were collected at 2 and 3 dpi, respectively. For CNV, *N. benthamiana* leaves were co-agroinfiltrated with $CNV^{20Kstop}$ (OD_{600} 0.4) and pGD-ATG11-Myc (OD_{600} 0.6) and pGD-P19 (OD_{600} 0.1), samples were collected at 2.5 dpai. NbATG11 protein level was determined by western blot assay using anti-myc antibody. Total RNA extraction and northern blot analyses were described above.

Confocal laser microscope studies in plants. To analyze the subcellular localization of NbATG11 in the presence or absence of viral components in *N. benthamiana* leaves, pGD-35S-T33-BFP, pGD-35S-C36-BFP, pGD-35S-RFP-NbATG11, pGD-35S-RFP-NbATG11-S1, pGD-35S-

RFP-NbATG11-R2, pGD-35S-GFP-SKL (as a peroxisome marker) and pGD-35S-GFP-AtTim21 (as a mitochondrial marker) (Xu and Nagy, 2016) were transformed into agrobacterium strain C58C1. Then, agrobacterium suspensions with different combinations were infiltrated into *N. benthamiana* leaves, followed by virus inoculation with sap at 16 h post agroinfiltration. At 2.5 dpai, the agroinfiltrated leaves were subjected to confocal laser microscopy (Olympus FV1200 and FV3000).

To detect interaction of NbATG11 with TBSV p33 or CIRV p36 replication proteins using bimolecular fluorescence complementation assay (BiFC), pGD-35S-T33-cYFP, pGD-35S-C36-cYFP, pGD-35S-C-cYFP (as a negative control), pGD-35S-nYFP-NbATG11, pGD-35S-nYFP-NbATG11-R2, pGD-35S-nYFP-MBP (as a negative control), pGD-35S-RFP-SKL (as a peroxisome marker) and pGD-35S-RFP-AtTim21 (as a mitochondrial marker) were transformed into agrobacterium strain C58C1. The Agrobacterium transformants with different combinations were used to infiltrate *N. benthamiana* leaves, followed by virus inoculation with sap at 16 h post agroinfiltration. At 2.5 dpai, the agroinfiltrated leaves were subjected to confocal laser microscopy.

To test if NbATG11 interacts with AtSac1 in the presence or absence of virus infection, *N. benthamiana* leaves were co-agroinfiltrated with pGD-35S-nYFP-NbATG11, pGD-35S-AtSac1-cYFP and either a combination of pGD-35S-T33-BFP and pGD-35S-RFP-SKL or pGD-35S-C36-BFP and pGD-35S-RFP-AtTim21. The agro-infiltrated *N. benthamiana* leaves at 16 hpai were inoculated with TBSV and CIRV sap, respectively, and then were subjected to confocal laser microscopy at 2.5 dpai.

Protein co-purification assays. The FLAG-tag based replicase purification from detergent-solubilized membrane fraction of yeast was performed as described (Li et al., 2008). In brief, plasmids HpGBK-CUP1-Hisp33/Gal-DI-72 and LpGAD-CUP1-His92 (as a control) or HpGBK-CUP1-Flagp33/Gal-DI-72 and LpGAD-CUP1-Flag92 were co-transformed with UpYES2-HisATG11 into BY4741. To determine recruitment efficiency of MCS-associated proteins by TBSV p33 into VROs in the presence or absence of Atg11, HpGBK-CUP1-Flagp33/Gal-DI-72 and LpGAD-CUP1-Flag92 were co-transformed with UpYC-Osh6, UpYC-Scs2, UpYC-Fis1 and UpYC-Sac1 respectively into BY4741 and atg11Δ yeasts. All transformed yeast cells were pre-grown in SC-ULH$^-$ media supplemented with 2% glucose and 100 μM BCS at 29 °C for 16 h. Then yeast cultures were re-suspended in SC-ULH$^-$ medium supplemented with 2% galactose and 100 μM BCS and grown at 23 °C for 24 h, followed by culturing yeast cells in SC-ULH$^-$ medium supplemented with 2% galactose and 50 μM $CuSO_4$ at 23 °C for 6 h. The cultures were resuspended and incubated in 35 ml phosphate-buffered saline (PBS) buffer containing 1% formaldehyde for 1 h on ice to cross-link proteins. Then, glycine (to 0.1 M) was added to quench the formaldehyde and the yeasts were incubated on ice for 5 min. Finally, yeast pellets were harvested after washing twice with PBS buffer and proteins were FLAG affinity-purified as described previously (Li et al., 2008).

For the pull down assay (Barajas et al., 2009), 100 μl crude lysate containing MBP, MBP-p33C (of TBSV) or MBP-p36C (of CIRV) were incubated with 20 μl amylose resin at 4 °C for 1 h. Then, the columns were washed with 800 μl washing buffer twice and then further incubated with the same amount of affinity-purified GST-His_6-ATG11 at 4 °C for 1 h. After incubation, the bound proteins from the columns were eluted with 30 μl SDS-loading buffer, followed by boiling the samples for 10 min prior to loading to PAGE.

Protein proximity-labeling assay in yeasts. To detect close proximity of p33 replication protein and Atg11 in yeasts, we transformed plasmids LpGAD-Gal-p92, UpYC-Avi-ATG11 (Avi-tag: GLNDIFEAQKIEWHW; a biotin acceptor) (Jan et al., 2014) and LpESC-His-Gal-BirA-p33-Gal10-DI72 (or pESC-His-Gal-p33-Gal10-DI72 as control) into BY4741 yeast strain. Transformed yeasts were pre-grown in 20 ml SC-ULH$^-$ media supplemented with 2% glucose at 29 °C for 20 h, followed by culturing yeast cells in 30 ml SC-ULH$^-$ media supplemented with 2% galactose at 23 °C for 24 h. Subsequently, 500 nM Biotin were added to the yeast cultures, followed by shaking at 29 °C for 2 h. The yeast cultures were centrifuged and washed with 1 × phosphate buffer saline (PBS). Then, the yeast cells were harvested and broken by glass beads and the membrane-fraction was solubilized by treatment with Triton X-100 as described (Li et al., 2008). The solubilized membrane fractions were added to the column filled with anti-strep-Tactin agarose to capture biotinylated proteins (Strep-tactin resin, cat# No.2-1201-002 from IBA) according to manufacturer's recommendations. The captured proteins were eluted in SDS-loading dye, followed by treatment in a heat block at 100 °C for 5 min. The purified Avi-Atg11 was detected by western-blotting with AP-conjugated anti--strep antibody.

To detect close proximity of p33 replication protein to the vMCS-associated proteins Osh6, Sac1, Scs2 and Fis1 in yeasts, we transformed plasmids LpGAD-Gal-p92 and LpESC-His-Gal-BirA-p33-Gal10-DI72 with one of the following plasmids: UpYC-Osh6-Avi, UpYC-Avi-Sac1, UpYC-Avi-Fis1 and UpYC-Avi-Scs2 into BY4741 yeast strain. Transformed yeast cells were grown in 2 ml SC-ULH$^-$ media supplemented with 2% galactose at 29 °C for 24 h. Then 250 nM Biotin were added to cultures, followed by growing the yeast cultures at 29 °C for 30 min. Biotinylated proteins were detected by western-blotting using AP-conjugated anti-strep antibody.

To determine if overexpression of Atg11 enhances the proximity of p33 replication protein to these vMCS-associated proteins, plasmids HpESC-His-Gal-BirA-p33-Gal10-DI72 and LpESC-Cup-ScATG11 (LpESC-Cup-EV as control) were co-transformed with either UpYC-Osh6-Avi or UpYC-Avi-Scs2 into yeast strain BY4741-p92 (expressing $p92^{pol}$ from a chromosomal location (Kovalev et al., 2012). Transformed yeast cells were grown in 2 ml SC-ULH$^-$ media supplemented with 2% galactose and 50 μM $CuSO_4$ at 29 °C for 24 h. Then 250 nM Biotin were added to cultures, followed by growing the yeast culture at 29 °C for 30 min. Biotinylated vMCS proteins were detected by western-blotting using anti-strep antibody.

To detect close proximity of Atg11 to the vMCS-associated proteins Osh6, Sac1, Scs2 and Fis1 in yeast in the presence or absence of viral replication proteins, plasmids LpESC-Gal-BirA-ATG11 and HpGBK-CUP1-Hisp33/Gal10-DI72, (or HpESC-Gal-EV as control) were co-transformed with one of the following plasmids: UpYC-Osh6-Avi, UpYC-Avi-Sac1, UpYC-Avi-Fis1 and UpYC-Avi-Scs2 into yeast strain BY4741-p92. Transformed yeast cells were grown in 2 ml SC-ULH$^-$ media supplemented with 2% galactose and 50 μM $CuSO_4$ at 29 °C for 24 h. Then, 250 nM Biotin were added to cultures, followed by growing the yeast culture at 29 °C for 30 min. Biotinylated vMCS proteins were detected by western-blotting using anti-strep antibody.

For time course assay, we transformed plasmids LpGAD-Gal-p92, UpYC-Osh6-Avi and HpESC-His-Gal-BirA-p33-Gal10-DI72 into BY4741 and atg11Δ yeast strains, respectively. Transformed yeast cells were pre-grown in 2 ml SC-ULH$^-$ media supplemented with 2% glucose at 29 °C for 16 h and then cultured yeast cells were washed and resuspended in 2 ml SC-ULH$^-$ media supplemented with 2% galactose with 250 nM Biotin. The yeast cultures were grown at 29 °C for 6 h, 12 h, and 24 h, followed by detecting the biotinylated Osh6 protein via western-blotting using anti-strep antibody.

Protein proximity-labeling assay in plants. To detect the close proximity of p33 replication protein and Atg11 in plants, *N. benthamiana* leaves were agroinfiltrated with pGD-p33-His-BirA (OD_{600} 0.4), pGD-NbATG11-HA-Avi (OD_{600} 0.4) and pGD-P19 (OD_{600} 0.2). Agroinfiltration with pGD-NbATG11-Myc (OD_{600} 0.4) and pGD-p33-His (OD_{60} 0.4) was used as a control. The infiltrated leaves at 3 dpai were further infiltrated with 200 μM Biotin. Then the infiltrated leaves after 40 min of biotin treatment were harvested and subjected to protein extraction. Biotinylated Atg11-HA-Avi protein was detected by western blotting using anti-strep antibody. Reciprocal experiments were done via agroinfiltration of *N. benthamiana* leaves with pGD-NbATG11-His-BirA (OD_{600} 0.4), pGD-p33-HA-Avi (OD_{600} 0.4) and pGD-P19 (OD_{600} 0.2). Agroinfiltration with pGD-ATG11-Myc (OD_{600} 0.4) was used as a control. Biotinylated p33-HA-Avi protein was detected by western

blotting using AP-conjugated anti-strep antibody.

To test if virus infection might affect close proximity of vMCS proteins and Atg11 in plants, we agroinfiltrated *N. benthamiana* leaves with pGD-P19 (OD_{600} 0.1), pGD-NbATG11-His-BirA (OD_{600} 0.3) and either pGD-Avi-His-AtORP3 (OD_{600} 0.3) or pGD-Avi-His-AtPVA12 (OD_{600} 0.3) with or without pGD-$CNV^{20KSTOP}$ (OD_{600} 0.3). We tested three different time points, namely 31 h, 48 h, and 56 h via infiltration with 200 μM Biotin at each time point. Then the infiltrated leaves after 40 min of biotin treatment were harvested and subjected to protein extraction. The biotinylated vMCS proteins were detected by western blotting using AP-conjugated anti-strep antibody.

Detection of Ergosterol distribution in yeasts. BY4741 and atg11Δ yeast strains were transformed with plasmids HpESC-Gal-Hisp33/Gal10-DI72, LpGAD-Gal-Hisp92 and UpYES2-ATG11 (or UpYES2-NT as a control). Filipin dye-staining was used to visualize ergosterol in yeast cells as described (Barajas et al., 2014b). Fixed yeast cells (2 μl resuspend cultures) were spotted onto a poly-Lysine coated slide and examined in the ZEISS UV light microscope with the DAPI filter set.

CRediT authorship contribution statement

Yuanrong Kang: Conceptualization, Methodology, Software, Data curation, Writing – original draft, Visualization, Investigation, Software, Validation. **Wenwu Lin:** Conceptualization, Methodology, Software, Data curation, Writing – original draft, Visualization, Investigation, Software, Validation. **Yuyan Liu:** Visualization, Investigation. **Peter D. Nagy:** Data curation, Writing – original draft, Supervision, Writing – review & editing, Writing – review & editing.

Acknowledgement

The authors are grateful to Drs. Judit Pogany and Shifeng Zhu for helping the project and helpful discussions. The authors acknowledge the initial contribution by Dr. N. Kovalev to adapt the protein proximity labeling approach. The authors thank Dr. J. Weismann (UCSF) for providing plasmids pJW1506 and pJW1234. This work was supported by the National Science Foundation (MCB-1517751 and IOS-1922895), USDA (NIFA, 2020-70410-32901) and a USDA hatch grant (KY012042) to PDN.

Appendix A. Supplementary data

Supplementary data to this article can be found online at https://doi.org/10.1016/j.virol.2022.04.007.

References

Altan-Bonnet, N., 2017. Lipid tales of viral replication and transmission. Trends Cell Biol. 27, 201–213.
Bachan, S., Dinesh-Kumar, S.P., 2012. Tobacco rattle virus (TRV)-based virus-induced gene silencing. Methods Mol. Biol. 894, 83–92.
Backues, S.K., Klionsky, D.J., 2012. Atg11: a Rab-dependent, coiled-coil membrane protein that acts as a tether for autophagy. Autophagy 8, 1275–1278.
Barajas, D., Li, Z., Nagy, P.D., 2009. The Nedd4-type Rsp5p ubiquitin ligase inhibits tombusvirus replication by regulating degradation of the p92 replication protein and decreasing the activity of the tombusvirus replicase. J. Virol. 83, 11751–11764.
Barajas, D., Martin, I.F., Pogany, J., Risco, C., Nagy, P.D., 2014a. Noncanonical role for the host Vps4 AAA+ ATPase ESCRT protein in the formation of Tomato bushy stunt virus replicase. PLoS Pathog. 10, e1004087.
Barajas, D., Xu, K., de Castro Martin, I.F., Sasvari, Z., Brandizzi, F., Risco, C., Nagy, P.D., 2014b. Co-opted oxysterol-binding ORP and VAP proteins channel sterols to RNA virus replication sites via membrane contact sites. PLoS Pathog. 10, e1004388.
Beh, C.T., Cool, L., Phillips, J., Rine, J., 2001. Overlapping functions of the yeast oxysterol-binding protein homologues. Genetics 157, 1117–1140.
Belov, G.A., van Kuppeveld, F.J., 2012. (+)RNA viruses rewire cellular pathways to build replication organelles. Curr Opin Virol 2, 740–747.
Chuang, C., Barajas, D., Qin, J., Nagy, P.D., 2014. Inactivation of the host lipin gene accelerates RNA virus replication through viral exploitation of the expanded endoplasmic reticulum membrane. PLoS Pathog. 10, e1003944.
Delorme-Axford, E., Klionsky, D.J., 2015. A missing piece of the puzzle: atg11 functions as a scaffold to activate Atg1 for selective autophagy. Autophagy 11, 2139–2141.
Drinnenberg, I.A., Weinberg, D.E., Xie, K.T., Mower, J.P., Wolfe, K.H., Fink, G.R., Bartel, D.P., 2009. RNAi in budding yeast. Science 326, 544–550.
Eickhorst, C., Licheva, M., Kraft, C., 2020. Scaffold proteins in bulk and selective autophagy. Progress in molecular biology and translational science 172, 15–35.
Feng, Z., Inaba, J.I., Nagy, P.D., 2021. Tombusviruses target a major crossroad in the endocytic and recycling pathways via Co-opting Rab7 mall GTPase. J. Virol. 95, e0107621.
Feng, Z., Kovalev, N., Nagy, P.D., 2020. Key interplay between the co-opted sorting nexin-BAR proteins and PI3P phosphoinositide in the formation of the tombusvirus replicase. PLoS Pathog. 16, e1009120.
Feng, Z., Xu, K., Kovalev, N., Nagy, P.D., 2019. Recruitment of Vps34 PI3K and enrichment of PI3P phosphoinositide in the viral replication compartment is crucial for replication of a positive-strand RNA virus. PLoS Pathog. 15, e1007530.
Fernandez de Castro, I., Fernandez, J.J., Barajas, D., Nagy, P.D., Risco, C., 2017. Three-dimensional imaging of the intracellular assembly of a functional viral RNA replicase complex. J. Cell Sci. 130, 260–268.
Fernandez de Castro, I., Tenorio, R., Risco, C., 2016. Virus assembly factories in a lipid world. Curr Opin Virol 18, 20–26.
Fernández-Suárez, M., Chen, T.S., Ting, A.Y., 2008. Protein-protein interaction detection in vitro and in cells by proximity biotinylation. J. Am. Chem. Soc. 130, 9251–9253.
Fukuda, T., Kanki, T., 2018. Mechanisms and physiological roles of mitophagy in yeast. Mol. Cell 41, 35–44.
Garcia-Ruiz, H., 2018. Susceptibility genes to plant viruses. Viruses 10, 484.
Gunawardene, C.D., Donaldson, L.W., White, K.A., 2017. Tombusvirus polymerase: structure and function. Virus Res. 234, 74–86.
Henne, W.M., 2016. Organelle remodeling at membrane contact sites. J. Struct. Biol. 196, 15–19.
Hsu, N.Y., Ilnytska, O., Belov, G., Santiana, M., Chen, Y.H., Takvorian, P.M., Pau, C., van der Schaar, H., Kaushik-Basu, N., Balla, T., Cameron, C.E., Ehrenfeld, E., van Kuppeveld, F.J., Altan-Bonnet, N., 2010. Viral reorganization of the secretory pathway generates distinct organelles for RNA replication. Cell 141, 799–811.
Hyodo, K., Okuno, T., 2020. Hijacking of host cellular components as proviral factors by plant-infecting viruses. Adv. Virus Res. 107, 37–86.
Inaba, J.I., Nagy, P.D., 2018. Tombusvirus RNA replication depends on the TOR pathway in yeast and plants. Virology 519, 207–222.
Inaba, J.I., Xu, K., Kovalev, N., Ramanathan, H., Roy, C.R., Lindenbach, B.D., Nagy, P.D., 2019. Screening Legionella effectors for antiviral effects reveals Rab1 GTPase as a proviral factor coopted for tombusvirus replication. Proc. Natl. Acad. Sci. U. S. A. 116, 21739–21747.
Jaag, H.M., Nagy, P.D., 2009. Silencing of Nicotiana benthamiana Xrn4p exoribonuclease promotes tombusvirus RNA accumulation and recombination. Virology 386, 344–352.
Jackson, C.L., Walch, L., Verbavatz, J.M., 2016. Lipids and their trafficking: an integral part of cellular organization. Dev. Cell 39, 139–153.
Jan, C.H., Williams, C.C., Weissman, J.S., 2014. Principles of ER cotranslational translocation revealed by proximity-specific ribosome profiling. Science 346, 1257521.
Janke, C., Magiera, M.M., Rathfelder, N., Taxis, C., Reber, S., Maekawa, H., Moreno-Borchart, A., Doenges, G., Schwob, E., Schiebel, E., Knop, M., 2004. A versatile toolbox for PCR-based tagging of yeast genes: new fluorescent proteins, more markers and promoter substitution cassettes. Yeast 21, 947–962.
Jin, X., Cao, X., Wang, X., Jiang, J., Wan, J., Laliberté, J.F., Zhang, Y., 2018. Three-Dimensional architecture and biogenesis of membrane structures associated with plant virus replication. Front. Plant Sci. 9, 57.
Kang, S., Shin, K.D., Kim, J.H., Chung, T., 2018. Autophagy-related (ATG) 11, ATG9 and the phosphatidylinositol 3-kinase control ATG2-mediated formation of autophagosomes in Arabidopsis. Plant Cell Rep. 37, 653–664.
Kovalev, N., Barajas, D., Nagy, P.D., 2012. Similar roles for yeast Dbp2 and Arabidopsis RH20 DEAD-box RNA helicases to Ded1 helicase in tombusvirus plus-strand synthesis. Virology 432, 470–484.
Kovalev, N., Inaba, J.I., Li, Z., Nagy, P.D., 2017. The role of co-opted ESCRT proteins and lipid factors in protection of tombusviral double-stranded RNA replication intermediate against reconstituted RNAi in yeast. PLoS Pathog. 13, e1006520.
Kovalev, N., Pogany, J., Nagy, P.D., 2019. Interviral recombination between plant, insect, and fungal RNA viruses: role of the intracellular Ca(2+)/Mn(2+) pump. J. Virol. 94.
Kovalev, N., Pogany, J., Nagy, P.D., 2020. Reconstitution of an RNA virus replicase in artificial giant unilamellar vesicles supports full replication and provides protection for the dsRNA replication intermediate. J. Virol. 94, e00267-20.
Laufman, O., Perrino, J., Andino, R., 2019. Viral generated inter-organelle contacts redirect lipid flux for genome replication. Cell 178, 275–289 e216.
Li, F., Vierstra, R.D., 2014. Arabidopsis ATG11, a scaffold that links the ATG1-ATG13 kinase complex to general autophagy and selective mitophagy. Autophagy 10, 1466–1467.
Li, Z., Barajas, D., Panavas, T., Herbst, D.A., Nagy, P.D., 2008. Cdc34p ubiquitin-conjugating enzyme is a component of the tombusvirus replicase complex and ubiquitinates p33 replication protein. J. Virol. 82, 6911–6926.
Li, Z., Pogany, J., Panavas, T., Xu, K., Esposito, A.M., Kinzy, T.G., Nagy, P.D., 2009. Translation elongation factor 1A is a component of the tombusvirus replicase complex and affects the stability of the p33 replication co-factor. Virology 385, 245–260.
Li, Z., Pogany, J., Tupman, S., Esposito, A.M., Kinzy, T.G., Nagy, P.D., 2010. Translation elongation factor 1A facilitates the assembly of the tombusvirus replicase and stimulates minus-strand synthesis. PLoS Pathog. 6, e1001175.

Lin, W., Feng, Z., Prasanth, K.R., Liu, Y., Nagy, P.D., 2021. Dynamic interplay between the co-opted Fis1 mitochondrial fission protein and membrane contact site proteins in supporting tombusvirus replication. PLoS Pathog. 17, e1009423.
Mäkinen, K., Lõhmus, A., Pollari, M., 2017. Plant RNA regulatory network and RNA granules in virus infection. Front. Plant Sci. 8, 2093.
Mao, K., Wang, K., Liu, X., Klionsky, D.J., 2013. The scaffold protein Atg11 recruits fission machinery to drive selective mitochondria degradation by autophagy. Dev. Cell 26, 9–18.
Matscheko, N., Mayrhofer, P., Rao, Y., Beier, V., Wollert, T., 2019. Atg11 tethers Atg9 vesicles to initiate selective autophagy. PLoS Biol. 17, e3000377.
Mesmin, B., Antonny, B., 2016. The counterflow transport of sterols and PI4P. Biochim. Biophys. Acta 1861, 940–951.
Molho, M., Lin, W., Nagy, P.D., 2021. A novel viral strategy for host factor recruitment: the co-opted proteasomal Rpn11 protein interaction hub in cooperation with subverted actin filaments are targeted to deliver cytosolic host factors for viral replication. PLoS Pathog. 17, e1009680.
Nagy, P.D., 2015. Viral sensing of the subcellular environment regulates the assembly of new viral replicase complexes during the course of infection. J. Virol. 89, 5196–5199.
Nagy, P.D., 2016. Tombusvirus-host interactions: Co-opted evolutionarily conserved host factors take center court. Annu Rev Virol 3, 491–515.
Nagy, P.D., 2017. Exploitation of a surrogate host, Saccharomyces cerevisiae, to identify cellular targets and develop novel antiviral approaches. Curr Opin Virol 26, 132–140.
Nagy, P.D., 2020. Host protein chaperones, RNA helicases and the ubiquitin network highlight the arms race for resources between tombusviruses and their hosts. Adv. Virus Res. 107, 133–158.
Nagy, P.D., Feng, Z., 2021. Tombusviruses orchestrate the host endomembrane system to create elaborate membranous replication organelles. Curr Opin Virol 48, 30–41.
Nagy, P.D., Pogany, J., 2012. The dependence of viral RNA replication on co-opted host factors. Nat. Rev. Microbiol. 10, 137–149.
Nagy, P.D., Pogany, J., Lin, J.Y., 2014. How yeast can be used as a genetic platform to explore virus-host interactions: from 'omics' to functional studies. Trends Microbiol. 22, 309–316.
Nagy, P.D., Strating, J.R., van Kuppeveld, F.J., 2016. Building viral replication organelles: close encounters of the membrane types. PLoS Pathog. 12, e1005912.
Nicholson, B.L., White, K.A., 2014. Functional long-range RNA-RNA interactions in positive-strand RNA viruses. Nat. Rev. Microbiol. 12, 493–504.
Oku, M., Sakai, Y., 2016. Pexophagy in yeasts. Biochim. Biophys. Acta 1863, 992–998.
Olkkonen, V.M., Li, S., 2013. Oxysterol-binding proteins: sterol and phosphoinositide sensors coordinating transport, signaling and metabolism. Prog. Lipid Res. 52, 529–538.
Panavas, T., Nagy, P.D., 2003. Yeast as a model host to study replication and recombination of defective interfering RNA of Tomato bushy stunt virus. Virology 314, 315–325.
Panaviene, Z., Panavas, T., Serva, S., Nagy, P.D., 2004. Purification of the cucumber necrosis virus replicase from yeast cells: role of coexpressed viral RNA in stimulation of replicase activity. J. Virol. 78, 8254–8263.
Paul, D., Bartenschlager, R., 2015. Flaviviridae replication organelles: oh, what a tangled web we weave. Annu Rev Virol 2, 289–310.
Pogany, J., Nagy, P.D., 2012. p33-Independent activation of a truncated p92 RNA-dependent RNA polymerase of Tomato bushy stunt virus in yeast cell-free extract. J. Virol. 86, 12025–12038.
Pogany, J., Nagy, P.D., 2015. Activation of Tomato bushy stunt virus RNA-dependent RNA polymerase by cellular heat shock protein 70 is enhanced by phospholipids in vitro. J. Virol. 89, 5714–5723.
Pogany, J., White, K.A., Nagy, P.D., 2005. Specific binding of tombusvirus replication protein p33 to an internal replication element in the viral RNA is essential for replication. J. Virol. 79, 4859–4869.
Prasanth, K.R., Kovalev, N., de Castro Martin, I.F., Baker, J., Nagy, P.D., 2016. Screening a yeast library of temperature-sensitive mutants reveals a role for actin in tombusvirus RNA recombination. Virology 489, 233–242.
Raiborg, C., Wenzel, E.M., Pedersen, N.M., Stenmark, H., 2016. Phosphoinositides in membrane contact sites. Biochem. Soc. Trans. 44, 425–430.
Sasvari, Z., Gonzalez, P.A., Rachubinski, R.A., Nagy, P.D., 2013. Tombusvirus replication depends on Sec39p endoplasmic reticulum-associated transport protein. Virology 447, 21–31.
Sasvari, Z., Kovalev, N., Gonzalez, P.A., Xu, K., Nagy, P.D., 2018. Assembly-hub function of ER-localized SNARE proteins in biogenesis of tombusvirus replication compartment. PLoS Pathog. 14, e1007028.
Sasvari, Z., Lin, W., Inaba, J.I., Xu, K., Kovalev, N., Nagy, P.D., 2020. Co-opted cellular Sac1 lipid phosphatase and PI(4)P phosphoinositide are key host factors during the biogenesis of the tombusvirus replication compartment. J. Virol. 94.
Schoggins, J.W., Randall, G., 2013. Lipids in innate antiviral defense. Cell Host Microbe 14, 379–385.
Sharma, M., Sasvari, Z., Nagy, P.D., 2010. Inhibition of sterol biosynthesis reduces tombusvirus replication in yeast and plants. J. Virol. 84, 2270–2281.
Sharma, M., Sasvari, Z., Nagy, P.D., 2011. Inhibition of phospholipid biosynthesis decreases the activity of the tombusvirus replicase and alters the subcellular localization of replication proteins. Virology 415, 141–152.
Shulla, A., Randall, G., 2016. (+) RNA virus replication compartments: a safe home for (most) viral replication. Curr. Opin. Microbiol. 32, 82–88.
van der Schaar, H.M., Dorobantu, C.M., Albulescu, L., Strating, J., van Kuppeveld, F.J.M., 2016. Fat(al) attraction: picornaviruses usurp lipid transfer at membrane contact sites to create replication organelles. Trends Microbiol. 24, 535–546.
Wang, A., 2015. Dissecting the molecular network of virus-plant interactions: the complex roles of host factors. Annu. Rev. Phytopathol. 53, 45–66.
Wang, X., Diaz, A., Hao, L., Gancarz, B., den Boon, J.A., Ahlquist, P., 2011. Intersection of the multivesicular body pathway and lipid homeostasis in RNA replication by a positive-strand RNA virus. J. Virol. 85, 5494–5503.
Xu, K., Nagy, P.D., 2014. Expanding use of multi-origin subcellular membranes by positive-strand RNA viruses during replication. Curr Opin Virol 9C, 119–126.
Xu, K., Nagy, P.D., 2015. RNA virus replication depends on enrichment of phosphatidylethanolamine at replication sites in subcellular membranes. Proc. Natl. Acad. Sci. U. S. A. 112, E1782–E1791.
Xu, K., Nagy, P.D., 2016. Enrichment of phosphatidylethanolamine in viral replication compartments via Co-opting the endosomal Rab5 small GTPase by a positive-strand RNA virus. PLoS Biol. 14, e2000128.
Xu, K., Nagy, P.D., 2017. Sterol binding by the tombusviral replication proteins is essential for replication in yeast and plants. J. Virol. 91.
Yokota, H., Gomi, K., Shintani, T., 2017. Induction of autophagy by phosphate starvation in an Atg11-dependent manner in Saccharomyces cerevisiae. Biochem. Biophys. Res. Commun. 483, 522–527.
Zhang, Z., He, G., Filipowicz, N.A., Randall, G., Belov, G.A., Kopek, B.G., Wang, X., 2019. Host lipids in positive-strand RNA virus genome replication. Front. Microbiol. 10, 286.
Zientara-Rytter, K., Subramani, S., 2020. Mechanistic insights into the role of Atg11 in selective autophagy. J. Mol. Biol. 432, 104–122.